Rational design, synthesis and pharmacological evaluation of a cohort of beta-adrenergic receptors ligands enables assessment of structure-activity relationships

Jacopo Tricomi,[a] Luca Landini,[a] Valentina Nieddu,[b] Ugo Cavallaro,[b] Jillian Baker,[c] Athanasios Papakyriakou,[d,*] Barbara Richichi.[a,*]

[a] Department of Chemistry, University of Firenze, Via della Lastruccia 13, 50019 Sesto Fiorentino (Firenze, Italy)

[b] Unit of Gynaecological Oncology Research, European Institute of Oncology IRCCS, Milan, Italy

[c] Cell Signalling Research Group, School of Life Sciences, University of Nottingham, Nottingham, NG7 2UH, UK.

[d] Institute of Biosciences and Applications, National Centre for Scientific Research "Demokritos", 15341 Agia Paraskevi, Athens, Greece

* Corresponding authors:

Athanasios Papakyriakou, thpap@bio.demokritos.gr

Barbara Richichi, barbara.richichi@unifi.it

In memory of Matteo Coveri (MC)

Keywords G-protein-coupled receptors, β-adrenergic receptors, aryloxy propanolamine, molecular docking, β-blocker, β-agonist, β-antagonist.

Abstract

Biomedical applications of molecules that are able to modulate β-adrenergic signaling have become increasingly attractive over the last decade, revealing that β-adrenergic receptors (β-ARs) are key targets for a plethora of therapeutic interventions, including cancer. Despite successes in β-AR drug discovery, identification of β-AR ligands that are useful as selective chemical tools in pharmacological studies of the three β-AR subtypes, or lead compounds for drug development is still a highly challenging task. This is mainly due to the intrinsic plasticity of β-ARs as G protein-coupled receptors in conjunction with the requirement for functional receptor subtype selectivity, tissue specificity and minimal off-target effects. With the aim to provide insight into structure-activity relationships for the three β-AR subtypes, we have synthesized and obtained the pharmacological profile of a series of structurally diverse compounds (named **MC**) that were designed based on the aryloxy-propanolamine scaffold of propranolol.

Comparative analysis of their predicted binding mode within the active and inactive states of the receptors in combination with their pharmacological profile revealed key structural elements that control their activity as agonists or antagonists, in addition to clues about substituents that mediate selectivity for one receptor subtype over the others. We anticipate that these results will facilitate selective β-AR drug development efforts.

1. Introduction

G-protein-coupled receptors (GPCRs) are a large and heterogeneous family (more than 800 members) of integral membrane proteins expressed in almost all human tissues[1,2] and they are involved in a plethora of human physiological processes.[3] They have several drug-able sites that are readily accessible at the cell surface, hence, it is not surprising that roughly 30% of drugs currently in the market target at least one GPCR.[4,5] Amongst them are the β-adrenergic receptors (β-ARs). They are comprised of three receptor subtypes (β1-AR, β2-AR and β3-AR) which share about 50% sequence homology within their transmembrane regions,[6] and are implicated in diverse physiological functions (*i.e.* heart rate and contractility, blood pressure, smooth muscle relaxation, lipolysis).[7,8] Recent advances in the structural characterization of β-ARs[9–15] that rely on static crystal structures, molecular dynamic simulations (MD) and advanced microscopy techniques (*i.e.* cryo-electron microscopy),[16,17] have allowed investigation into key features associated with β-AR activation and reveal details on the dynamic processes associated with G-protein stimulation (*i.e.* side-chain switches, the plasticity of transmembrane helices, receptor active/inactive states).[16,18–20] Notably, the availability to this vast amount of information has provided structural clues for ligand subtype selectivity, binding mode, and fingerprint interactions,[15,21–23] further allowing researchers to perform comparative docking calculations for structure-based drug design and virtual ligand screening.[13,24] Additionally, the key role of the conformation and type of amino acid residues of the extracellular loop 2 (ECL2) in the ligand binding and subtype selectivity has been recently elucidated.[12,22,25]

Despite successes in β-AR drug discovery in terms of drug availability in the market and promising results using different agents in clinical trials[4] the widespread expression of different β-ARs in the body still makes the elucidation of receptor

subtype, functionality (agonist *vs* antagonist *vs* inverse agonist), and selectivity of β-AR ligands a challenging issue in the identification of β-ARs targeted therapeutics with reduced off-target effects.[4,20] In addition, differences between rodent and human β-ARs, in particular the β3 subtype, render the identification of selective ligands a far more challenging task.[26,27] Notably, the biomedical applications for β-AR targeted agents are continuously expanding from the most common area of therapeutic intervention (*i.e.* asthma, cardiovascular diseases) into novel emerging areas (*i.e.* overactive bladder,[28] multiple sclerosis,[29] neurodegenerative disorders,[30] and cancer[31]). In particular, β2-AR and β3-AR have emerged as key players in cancer progression as they are significantly overexpressed in multiple tumor types[32] and their levels correlate with disease stage and prognosis.[33]

In the last decade, researchers have investigated the role of β-ARs in cancer by exploiting the pharmacologic antagonism of β-adrenergic signaling.[25,34,35]. In particular, the β2-AR is one of the best characterized GPCR and the availability of a significant set of X-ray structures of β2-AR complexes with different ligands has provided the template for *in silico* ligand docking and for the discovery of new β2-AR ligands.[13,15,36–40] In this regard, propranolol, the nonselective β1-/β2-blocker discovered in 1965[41] revolutionized the clinical management of angina pectoris,[42] and provided relevant insights to translational researchers on the role of the β2-AR signaling in various stages of cancer development.[33] On the other hand, β3-AR,[43–45] defined as the odd sibling of β-ARs,[46] is the last discovered adrenoreceptor subtype. Thus, information available for β3-ARs is far less when compared to β1- and β2-ARs,[47–50] and only recently has the transmission electron cryo-microscopy (cryo-TEM) structure of the β3-AR with the agonist Mirabegron complex [51] been reported.[12] This receptor was first utilized as a target for the treatment of obesity and/or diabetes owing to its ability to regulate lipolysis, and thermogenesis, and selective β3-AR agonists (*i.e.* Mirabegron, Vibegron) have been approved for the treatment for overactive bladder.[28,51] These are the only validated β3-AR ligand therapeutics in use as drug discovery on β3-AR blockers is more complicated.[34,48,52]

More recent reports indicate β3-AR as an attractive target for drug discovery in cancer models.[34,48,52] In particular, some authors[53–55] claimed an effect on tumor cell

proliferation, metabolism (*i.e.* Warburg effect), and on immune escape in adult and pediatric cancer models, which were linked to β3-AR blockade using the aryloxy-propanol-aminotetralin derivative SR59230A (Figure 1).[56] However, the initial assessment of SR59230A as selective β3-AR blocker on rat models [56] has been revised, and several investigators claim that this compound does not fill the criteria for a useful β3-AR selective antagonist in human cell models.[27,46–48,57,58]

All these findings provide strong evidence for continued efforts in β-AR drug development, with designs aimed at the identification of selective chemical tools either for the study of pharmacology and the biological effect in disease models, or their use as therapeutics. In this regard, functional and receptor subtype selectivity, tissue specificity, drug toxicity, and short plasma half-life are some of the issues that need to be addressed. Additionally, the main complication of limiting off-target effects due to the plasticity of β-AR affecting receptor subtype selectivity and ligand-directed signaling, namely the ability of β-AR ligands to direct the signaling toward one pathway or another according to the activation state and the conformation of the β-AR they bind.[20,59–61] Thus, selective stimulation of a single signaling pathway is a challenging goal that could ensure the translation of the results into clinics while mitigating undesirable side effects resulting from simultaneous activation of other pathways. All these obstacles emphasize the need for focusing efforts on the identification of further structural clues for β-AR activity/selectivity. In particular, the identification of new molecular entities may enable the in-depth exploration of the chemical space around the previously reported ligands, leading to insights into their structure−activity relationship.[13,25,62–64] In line with this, some objectives have been accomplished and have proven that the knowledge on structural diversity can assist in addressing the goal of performing an atomic level correlation between chemical structures and their activity toward β-ARs.

In an attempt to gain new insights into structure-activity/functional selectivity relationships we prepared a series of new β-AR ligands, **MC1**–**34** (Figure 1), which contain a common aryloxy propanolamine moiety. The design approach of these compounds is outlined in Figure 1 and is based on the introduction of different substitutions to either the R_1 or R_2 regions of the compound. On the left side of the MC derivatives a combination of diverse aryl moiety substitutions, named R_1 (Figure 1) were introduced, whereas on the right side of the compound different amine groups

are linked using a combination of various chemical entities, named R_2 (Figure 1). Therefore, we report here on the straightforward synthetic approach to prepare compounds **MC1**–**34** along with their pharmacological profile *vs* all the three β-ARs with the aim of understanding how agonist *vs* antagonist potency and selectivity could change by the presence of various chemical entities. To this end, comparative molecular docking calculations were employed using the three receptor subtypes with known agonists and antagonists.

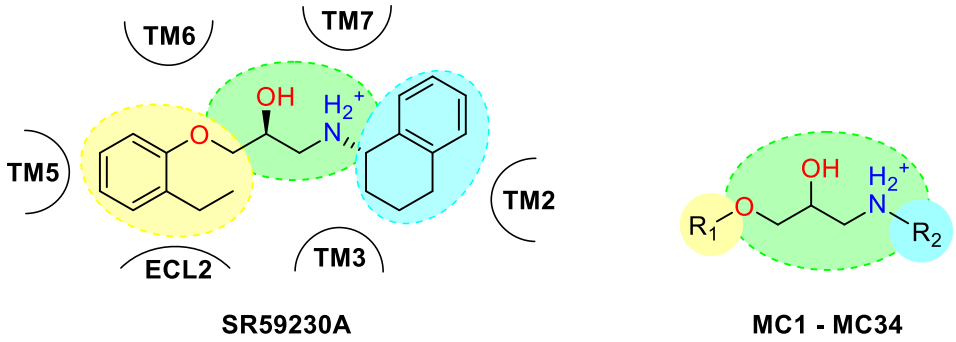

Figure 1. A schematic representation of the structure of SR59230A highlighting the common functional moieties of β-AR ligands with respect to their interactions at the orthosteric site, and the general structure of the **MC** derivatives prepared in this work.

2. Results and discussion

2.1 Structure-based design of the MC ligands

Our rational design of **MC** ligands encompasses all three β-ARs in both their active and inactive states. For β3-AR we used homology models based on the X-ray structures of β2-AR, whereas for β1-AR we employed the X-ray structures from the homologous receptor of wild turkey (see Computational Methods for detail). Docking was performed with FRED that employs the Chemgauss4 scoring function,[65,66] with a dense set of conformations for the ligands that was generated using OMEGA.[67,68] To obtain meaningful pose predictions, we applied H-bond restraints for residues $D^{3.32}$ as acceptor and $N^{7.39}$ as both donor and acceptor. In the aryloxy propanolamine series, the oxymethylene bridge in combination with more hydrophobic R_1 groups is a common feature of many β-AR antagonists and inverse agonists, whereas agonists engage more polar aryl groups directly linked to the ethanolamine moiety.[15,69] In particular, most full or partial agonists contain H-bond donors that interact with $S^{5.42}$ and $S^{5.46}$ in

transmembrane helix 5 (TM5), a feature that may be present in antagonists or inverse agonists albeit not optimal for H-bonding interactions.[70–72] The emerging insights on the role of SR59230A in cancer progression prompted us to investigate its interactions with all the β-ARs subtypes, and thus provided relevant structural details on its binding mode that supported our rationale. Docking results for SR59230A in both states of the 3 receptors and in comparison, with the X-ray structure of β2-AR with bound propranolol are illustrated in Figure 2. Our docking results with SR59230A suggest that it can bind the inactive states of the three β-ARs in a similar manner and with equal affinity (Figure 2C–E, and Supplementary Data, Table S1).

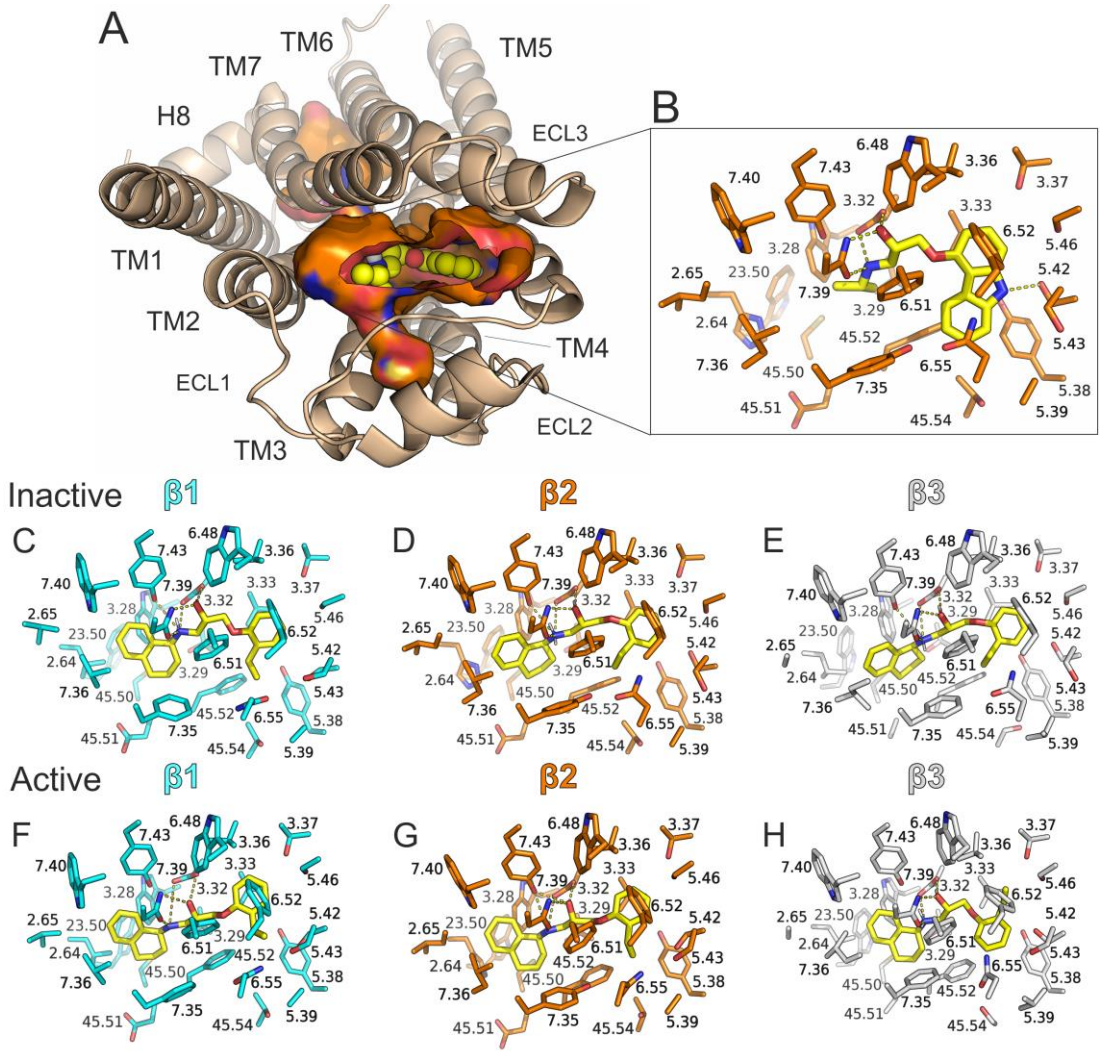

Figure 2. **(A)** Cartoon representation of β2-AR in the inactive state with *S*-propranolol bound (PDB ID: 6PS5).[73] The ligand is shown as spheres color-coded with yellow for C, red for O and blue for N, whereas the orthosteric site is shown with a surface. **(B)** Close-up view of the ligand-binding site illustrating all β2-AR residues that comprise the interaction fingerprint profile as revealed from a series of experimentally determined β1- and β2-AR complexes with

ligands.[69] *S*-propranolol is shown as sticks with yellow C atoms and hydrogen-bonding interactions are indicated with green dashed lines. (**C–E**) Predicted bound poses of SR59230A in the inactive states of β1-AR (residues in cyan C sticks), β2-AR (orange C) and β3-AR (grey C). The orientation of the binding site is similar to panel **B** in all receptors. (**F–H**) Predicted bound poses of SR59230A in the active states of β1-, β2- and β3-AR, respectively, illustrated in the same way as in panels **C**–**E**.

This is also the case for the active states of the β-ARs, although a rather lower score is estimated for β2- and β3-AR with respect to β1-AR (Figure 2F–H, Table S1). This suggests that SR59230A could act as an equally potent antagonist of not only β3-AR, but also β1- and β2-ARs. The central ethanolamine is docked properly to make polar interactions with $D^{3.32}$ and $N^{7.39}$, whereas the ethylbenzene group (R_1) is accommodated *via* hydrophobic contacts with the conserved residues $V^{3.33}$, $V^{3.36}$, $T^{3.37}$, $F^{45.52}$, $Y^{5.38}$, $F^{6.51}$ and exhibits an aromatic, T-shaped interaction with $F^{6.52}$. Notably, the tetralin group of SR59230 (R_2) is in contact with the ECL2[74] residues at position 45.50 (conserved C), 45.51 (D/D/A, for β1/β2/β3, respectively) and 45.52 (conserved F), the TM2 residue at 2.64 (L/H/L), and the TM7 residues at 7.35 (F/Y/F), 7.36 (V/I/L), 7.40 (W), in addition to a common T-shaped aromatic interaction with the conserved $Y^{7.43}$. It should be noted however that subtle conformational changes, even for conserved β-AR residues, gives rise to a small shift in the position and orientation of the central ethanolamine moiety. For SR59230A, the relative orientation of $W^{3.28}$ and $Y^{7.43}$ affect the exact placement of the bulky R_2 and as an effect, the orientation of ethanolamine. Therefore, as observed for SR59230A in the inactive state of β3- and β2-AR, the hydrogen bonding ability of the central amine with $D^{3.32}$ is lost (N–H···O angle < 120 deg, and/or N···O distance > 3.5 Å) and interacts only with $N^{7.39}$ (Figure 2C-D).

In our initial design, we employed structurally different substituted aryl groups in R_1 (both comprising the oxymethylene bridge, Scheme 1) with the aim to investigate their potential effect upon interaction with the conserved triad of polar serine residues at positions 5.42, 5.43 and 5.46 in TM5. These groups were combined with a series of R_2 residues (Scheme 1) bearing aryl groups that are linked *via* linear alkyl chains of 1–6 carbon atoms, which provide ligands with flexibility between β-AR residues of TM3 and TM7. Their pharmacological evaluation provided interesting results that will be discussed in conjunction with their predicted binding modes.

2.2 Synthesis of the MC ligands

MC1–**MC34** (Figure S1) have been prepared by following a synthetic strategy of only a few steps that takes advantage of commercially available reagents and allows for a wide range of chemical diversification in the R_1 and R_2 residues of the **MC** ligands. Several studies demonstrated that the stereochemistry of the stereogenic center bearing the hydroxyl group of the aryloxy propanolamine moiety affects the binding to the receptors.[72,75] In particular, in the aryloxy propanolamine series, the activity of the ligands is higher when the stereocenter has the (S) configuration. Accordingly, optically active reagents have been employed in the synthetic strategy that consists of two nucleophilic substitution reactions. At first, the epoxide derivatives **1**–**8** (Scheme 1) have been prepared by the reaction of the (S)-(+)-epichlorohydrin **9** with the commercially available phenol derivatives **1p**–**8p** (Scheme 1). In turn, epoxide derivatives **1–8** were bonded with the primary amine derivatives **10**–**19** (Scheme 1) providing the final compounds **MC1**–**34** by means of an epoxide ring opening route.

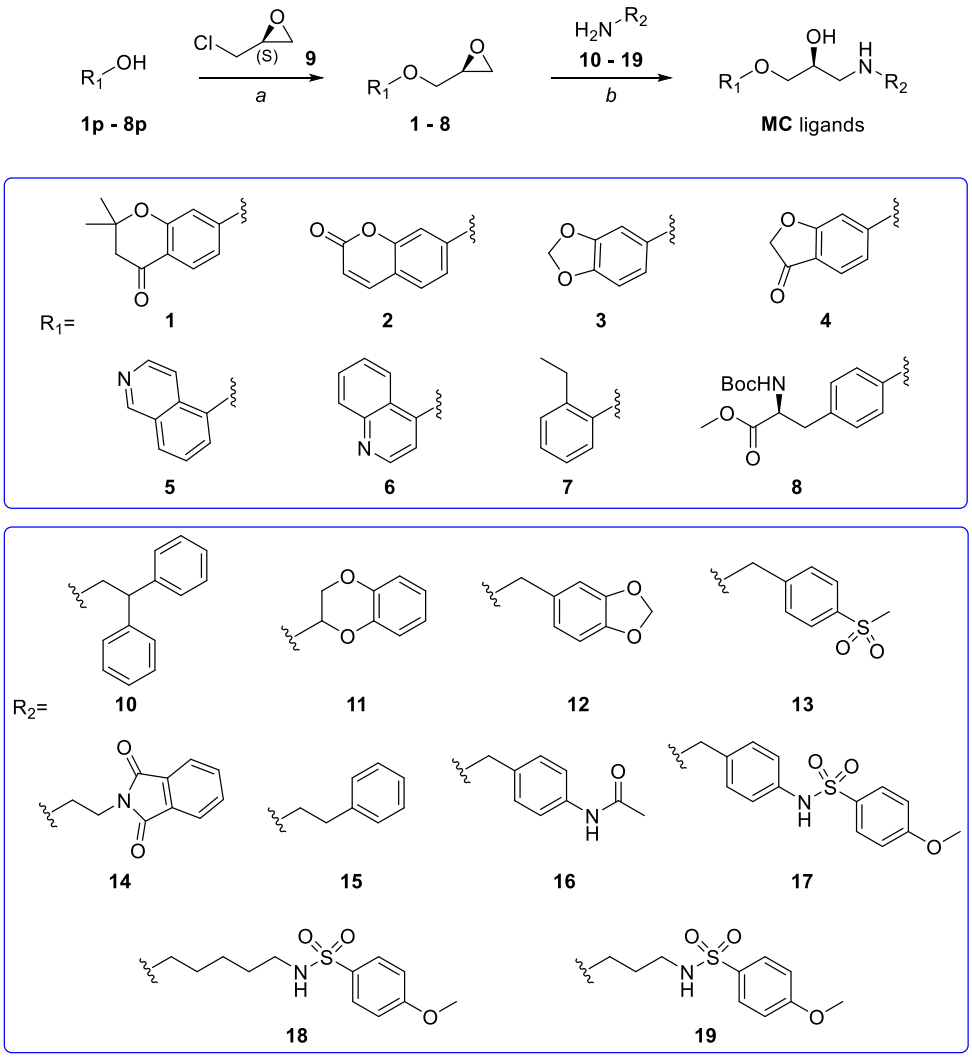

Scheme 1. Synthetic strategy employed in this work. Reaction conditions *a*: K_2CO_3, dry *N*,*N*-dimethylformamide, 50°C; (83% yield, **1**), (94% yield, **2**), (51% yield, **3**), (8% yield, **5**), (57% yield, **6**), (70% yield, **8**). *b*: see Table 1.

A general protocol for the synthesis of all the epoxide derivatives **1**–**8** studied in this work (Scheme 1, Table S2) was set up in mild experimental conditions (DMF, 50°C, K_2CO_3), creating the corresponding epoxides from good to high yields (Scheme 1) according to the phenol reagents used in the reaction. Phenols **1p**–**8p** were selected to ensure the hydrophobic interactions of the R_1 groups of the **MC** ligands with the TM5 and TM6 of β-ARs targeted at the development of antagonist, or inverse agonists. In addition, polar functional groups were also included, aimed at investigating their potential effects upon interaction with the conserved polar serine residues in TM5.

Indeed, as mentioned in the previous section, these types of interactions with TMs significantly affect the functional activity of the ligands to the β-ARs. Thus, commercially available phenol reagents can be placed onto the oxygen containing bicyclic derivatives **1p**–**4p** (*i.e.* chromanone, coumarin, sesamol and benzofuranone derivatives respectively), which have a common aryl group fused with an additional five- or six-member cycle and the nitrogen containing heterocyclic aromatic derivatives, such as the isomeric hydroxyquinolines **5p**–**6p**, respectively 5-hydroxyquinoline and 4-hydroxyquinoline (Scheme 1). Further, the 2-ethyl phenol **7p** provides the R_1-basedanalogue of SR59230A. Finally, the phenol **8p** is a protected derivative of the amino acid (L)-tyrosine. It was included in our study as a case of oxygen containing phenol derivatives where the oxygen atom is not included in an additional cycle. In **8p** the introduction of an amine group allows for further investigations of additional interactions with the TM5 and TM6 of the receptors (*i.e.* aromatic residues $Y^{5.38}$, $F^{6.51}$ and $F^{6.52}$).

The selected primary amines employed in the epoxide ring opening (Scheme 1) contain an aromatic hydrophobic group and diverse polar functionalities with the potential to form hydrogen bonds with the orthosteric binding site. The size and the conformation of the substituent at the nitrogen atom of the β-AR ligands significantly affect binding and selectivity *vs* the three β-ARs subtypes. Hence, the use of a combination of various chemical entities bearing at least one aromatic group (Scheme 1) was explored aiming to investigate the interactions between the R_2 substituents and the site of the β-ARs that is mainly involved in the activation of the intracellular

signaling. On this basis, either commercially available amines (**10**–**15**, Scheme 1), and synthetic amines (**16**–**19**, Scheme 1), easily obtainable in a few synthetic steps, were selected. Among them, amines **13**, **16** and **17** contain a benzyl group that is *p*-substituted with different polar functional groups (*i.e.* sulfonyl group, amide, and sulfonamide group). Amines **17**, **18** and **19** contain a common aryl sulfonamide group which is separated from the nitrogen atom by spacers of different length and flexibility.[25] The presence of bulky substituents (*i.e* **10**) and bicyclic derivatives (*i.e.* 1,4-benzodioxane, benzodioxole and phthalimide derivatives such as **11**, **12** and **14**) were also investigated.

Consequently, the outcome of epoxide ring opening reactions (Scheme 1) between the selected amino derivatives **10**–**19** and the epoxy derivatives **1**–**8** were strongly affected (Table 1) by the type and related reactivity of the substrates used (either the epoxide or the amine). A set of solvents were tested, and the use of 2-propanol allowed for obtaining higher yields (entries *e*–*j* and *l*–*r*, Table 1). In some cases, dimethylsulfoxide (entries *o*–*r*, Table 1) was used at different percentages (16–25%) according with the solubility of the reagents, whereas the triethylamine (entries *g*–*j* and *o*–*r*, Table 1) was employed as non-nucleophilic organic base.

Table 1. Reaction conditions: *i*: dry methanol; *ii*: dry dimethylformamide; *iii*: dry methanol, N-methylmorpholine; *iv*: dry 2-propanol, *N*,*N*-diisopropylethylamine; *v*: dry 2-propanol; *vi*: dry 2-propanol, triethylamine; *vii*: dry 2-propanol:dimethylsulfoxide 5:1, triethylamine; *viii*: dry 2-propanol:dimethylsulfoxide 3:1, triethylamine; *ix*: a) dry 2-propanol:dimethylsulfoxide 5:1, triethylamine, b) trifluoroacetic acid, dichloromethane. * The structure of all the MC ligands is reported in Figure S1.

Entry	Epoxide	Amine	Reaction conditions	Yield	MC*
a	**1**	**10**	*i*	30%	**2**
b	**1**	**11**	*i*	50%	**3**
c	**1**	**12**	*ii*	47%	**4**
d	**1**	**13**	*iii*	27%	**7**
e	**1**	**14**	*iv*	12%	**10**
f	**1**	**15**	*v*	94%	**11**
g	**1**	**16**	*vi*	91%	**26**
h	**1**	**17**	*vi*	64%	**28**
i	**1**	**18**	*vi*	25%	**30**
j	**1**	**19**	*vi*	28%	**32**
k	**2**	**11**	*i*	43%	**08**
l	**2**	**12**	*v*	78%	**21**
m	**2**	**13**	*iv*	65%	**09**
n	**2**	**14**	*iv*	37%	**20**
o	**2**	**16**	*vii*	53%	**27**

p	**2**	**17**	*vii*	69%	**29**
q	**2**	**18**	*viii*	13%	**31**
r	**2**	**19**	*viii*	18%	**33**
s	**3**	**10**	*i*	50%	**01**
a’	**3**	**11**	*vi*	28%	**22**
b’	**4**	**11**	*vi*	68%	**23**
c’	**5**	**11**	*vi*	67%	**24**
d’	**6**	**11**	*vi*	45%	**25**
e’	**8**	**11**	*ix*	26%	**34**

To further investigate the role of the stereochemistry of the hydroxyl group of the aryloxypropanolamine moiety of the MC ligands in the interaction with the β-ARs, a commercially available enantiomeric pure (R)-(–)-epichlorohydrin **9b** (Scheme S1 and Table S3) was employed in reactions with a selected set of amine derivatives (*i.e.* **10–15**, Scheme 1) affording the **MC14–19** ligands (Scheme S1 and Figure S1).

2.3 Pharmacological evaluation

The pharmacological profiles of compounds **MC1–34** was evaluated by monitoring the CRE-SPAP production on CHO cells stably transfected with the human β-ARs and a CRE-SPAP reporter gene, as previously reported.[13,27,62,76]

2.3.1 Agonist responses

Fenoterol (Figure S2) stimulated a CRE-SPAP full agonist response (with respect to isoprenaline) in the human CHO-β1, CHO-β2 and CHO-β3 cell lines (Table 2).

Table 2. Log EC_{50} and % response compared to that stimulated by 10μM isoprenaline determined in the same plate for agonist responses in the human CHO-β1, CHO-β2 and CHO-β3 cell lines. Values are mean ± SEM of n separate experiments. All ligands were assessed. Thus, apart from **MC1**, **MC2**, **MC22** and **MC24** the remaining MC compounds, ICI118551 and CGP20712A all had no response (n=3 or more separate experiments in each case, each to a maximum concentration of 10 μM). Where the top of the concentration curve was not reached (*e.g.* **MC1** at β3, Figure 3) it was not possible to obtain an EC_{50} and thus the stimulation as a % of isoprenaline at the highest concentration used is given. The chemical structures of all compounds are shown in Figures S1–S2**.**

	Human β1-AR			**Human β2-AR**			**Human β3-AR**		
	Log EC_{50}	% isop.	n	Log EC_{50}	% isop.	n	Log EC_{50}	% isop.	n
fenoterol	–7.96 ± 0.07	96.2 ± 3.0	12	–9.61 ± 0.07	100.3 ± 2.3	12	–7.66 ± 0.06	100.2 ± 2.8	11

L748337	–6.42 ± 0.11	63.6 ± 11.9	6	10 µM	3.7 ± 2.1	4	–8.35 ± 0.13	61.2 ± 4.9	5
SR59230A	–7.32 ± 0.10	60.8 ± 11.3	6	–8.06 ± 0.13	27.1 ± 5.7	3	–6.72 ± 0.03	63.7 ± 4.7	6
MC ligands									
MC1	–6.51 ± 0.06	67.7 ± 4.1	5	–6.86 ± 0.09	29.1 ± 2.9	5	3 µM	41.1 ± 3.0	6
MC2	–6.52 ± 0.13	48.8 ± 7.0	5	–6.95 ± 0.12	26.5 ± 1.7	6	3 µM	30.9 ± 4.1	5
MC4	No response		4	10 µM	17.5 ± 2.0	4	No response		4
MC22	–7.13 ± 0.15	23.3 ± 8.1	5	10 µM	14.2 ± 1.8	4	10 µM	14.7 ± 3.4	5
MC24	–6.50 ± 0.19	36.7 ± 5.5	4	No response		3	No response		4

L748337 and SR59230A (Figure 4) also stimulated agonist responses in CHO-β1, CHO-β2 and CHO-β3 cell lines although these were only partial responses (Table 2). In relation to isoprenaline (Table 2), the β2-response for L748337 was too small to determine an accurate EC_{50} value. Among MC derivatives, **MC1**, **MC2**, **MC22** and **MC24** (Table 2) also stimulated an agonist response, but no response was seen to any other of the MC compounds.

2.3.2 Antagonist affinity

The antagonist affinity (log K_D) of each ligand was assessed based on the ability to cause a rightward shift of the fenoterol concentration response curve (Table 3).

Table 3. Log K_D values obtained from a rightward shift of the fenoterol concentration response determined in the human CHO-β1, CHO-β2 and CHO-β3 cell lines. Values are mean ± SEM of n separate experiments. Where there was no shift in the fenoterol response curve, a K_D value could not be calculated and is given as >10 µM. The chemical structures of all compounds are shown in Figures S1–S2**.**

	Human β1		**Human β2**		**Human β3**	
	Log K_D	n	Log K_D	n	Log K_D	n
CGP 20712A	–8.99 ± 0.19	6	–5.70 ± 0.11	7	–5.13 ± 0.10	8
ICI 118551	–6.92 ± 0.11	7	–9.45 ± 0.04	7	–6.00 ± 0.06	8
L748337	–6.47 ± 0.13	4	–7.13 ± 0.17	7	–8.17 ± 0.15	7
SR59230A	–7.43 ± 0.16	6	–8.42 ± 0.14	7	–7.16 ± 0.16	9
MC ligands						
MC1	–6.87 ± 0.14	6	–7.73 ± 0.07	4	–6.37 ± 0.04	5
MC2	–6.59 ± 0.15	4	–7.20 ± 0.13	5	–6.16 ± 0.15	5
MC3	–5.44 ± 0.12	5	–5.21 ± 0.11	5	–5.10 ± 0.03	5
MC4	> 10 µM	5	> 10 µM	4	> 10 µM	4
MC7	> 10 µM	3	> 10 µM	3	> 10 µM	3
MC8	–5.62 ± 0.10	4	–5.18 ± 0.11	4	–5.59 ± 0.09	4

MC9	> 10 µM	4	> 10 µM	3	> 10 µM	3
MC10	> 10 µM	3	> 10 µM	3	> 10 µM	3
MC11	–5.41 ± 0.10	4	–5.64 ± 0.07	4	> 10 µM	4
MC14	–5.64 ± 0.06	4	–5.92 ± 0.10	4	> 10 µM	4
MC15	–5.51 ± 0.07	4	–5.30 ± 0.14	4	> 10 µM	4
MC16	–5.50 ± 0.05	4	–5.44 ± 0.10	4	> 10 µM	5
MC17	–5.78 ± 0.05	4	–6.14 ± 0.12	5	–5.06 ± 0.09	6
MC18	> 10 µM	3	> 10 µM	3	> 10 µM	3
MC19	> 10 µM	3	> 10 µM	3	> 10 µM	3
MC20	> 10 µM	3	> 10 µM	3	> 10 µM	3
MC21	–5.25 ± 0.10	4	–5.20 ± 0.18	4	> 10 µM	4
MC22	–6.99 ± 0.12	6	–6.97 ± 0.10	6	–5.87 ± 0.13	6
MC23	–5.22 ± 0.13	5	> 10 µM	4	–5.11 ± 0.11	5
MC24	–5.80 ± 0.07	6	–5.81 ± 0.09	6	–5.47 ± 0.06	6
MC25	–5.44 ± 0.19	5	–5.44 ± 0.15	5	–5.85 ± 0.13	5
MC26	–5.76 ± 0.09	5	> 10 µM	4	> 10 µM	4
MC27	–5.49 ± 0.17	5	> 10 µM	4	> 10 µM	4
MC28	> 10 µM	4	–5.51 ± 0.04	5	–5.92 ± 0.08	5
MC29	> 10 µM	4	–5.76 ± 0.13	5	–5.93 ± 0.03	5
MC30	> 10 µM	4	–5.85 ± 0.14	5	> 10 µM	4
MC31	> 10 µM	4	–5.80 ± 0.05	5	> 10 µM	4
MC32	> 10 µM	4	–6.07 ± 0.10	5	> 10 µM	4
MC33	> 10 µM	4	–5.94 ± 0.13	5	> 10 µM	4
MC34	> 10 µM	4	> 10 µM	4	> 10 µM	4

CGP20712A, a β1-selective antagonist and ICI118551 a β2-selective antagonist inhibited fenoterol responses (Table 3), but CGP20712A had high affinity at β1 (log K_D –8.99), ICI118551 had high affinity at β2 (log K_D –9.45), and both were low affinity at β3 in keeping with previous studies[26,27] and therefore confirming the presence of the three different β-ARs in of these cell line respectively (Table 3). SR59230A was not a β3-selective ligand for the human β-adrenoceptors in keeping with previously reported data[26,58] (Figure 4). The K_D values obtained here are also similar to the values obtained from radioligand binding studies (log K_D –7.54, –8.45 and –7.37 for β1, β2 and β3, Table 3).[58] **MC1** (Figure 3) had the highest affinity and retained the partial agonist nature of its parent SR59230A (Figure 4).

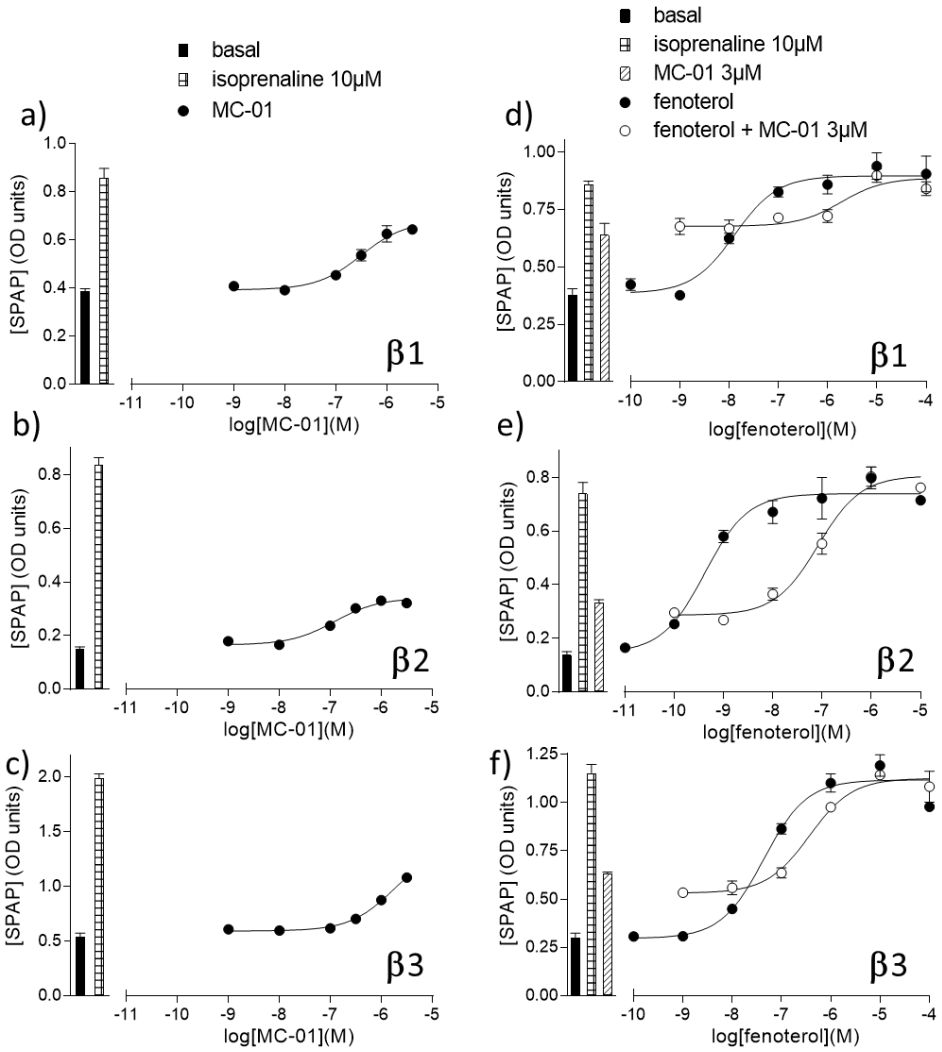

Figure 3. a–c) Concentration response curves for CRE-SPAP production by **MC1** in a) CHO-β1, b) CHO-β2 and c) CHO-β3 cells. Bars represent basal CRE-SPAP production and that in response to 10 μM isoprenaline; d–f) CRE-SPAP production in response to fenoterol in the absence and presence of 3μM **MC1** in d) CHO-β1, e) CHO-β2 and f) CHO-β3 cells. Bars represent basal CRE-SPAP production, that in response to 10 μM isoprenaline and that in response to 3μM **MC1** alone. Data are mean ± SEM of triplicate values and are representative of a) 5, b) 5, c) 6, d) 6, e) 4 and f) 5 separate experiments.

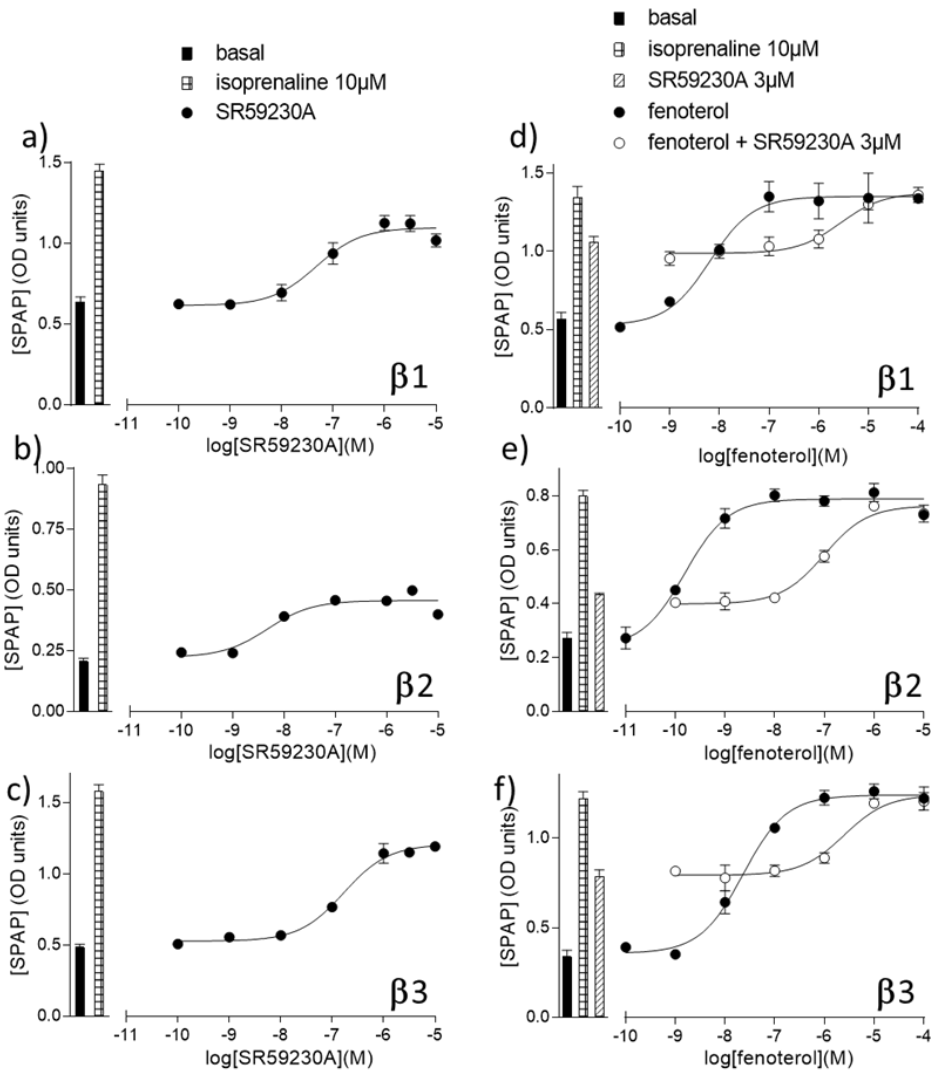

Figure 4. a–c) Concentration response curves for CRE-SPAP production by **SR59230A** in a) CHO-β1, b) CHO-β2 and c) CHO-β3 cells. Bars represent basal CRE-SPAP production and that in response to 10 μM isoprenaline; d–f) CRE-SPAP production in response to fenoterol in the absence and presence of 3μM SR59230A in d) CHO-β1, e) CHO-β2 and f) CHO-β3 cells. Bars represent basal CRE-SPAP production, that in response to 10 μM isoprenaline and that in response to 3μM **SR59230A** alone. Data are mean ± SEM of triplicate values and are representative of a) 6, b) 3, c) 6, d) 6, e) 7 and f) 9 separate experiments.

MC2 demonstrated a similar pharmacological profile, whereas its (R)-enantiomer **MC17** revealed a ten-fold lower affinity, and loss of agonist activity. Finally, **MC30–33** are β2-selective antagonists (Tables 2–3), whereas **MC28** (Figure 5) was the most β3-selective compound, although none had any agonist activity.

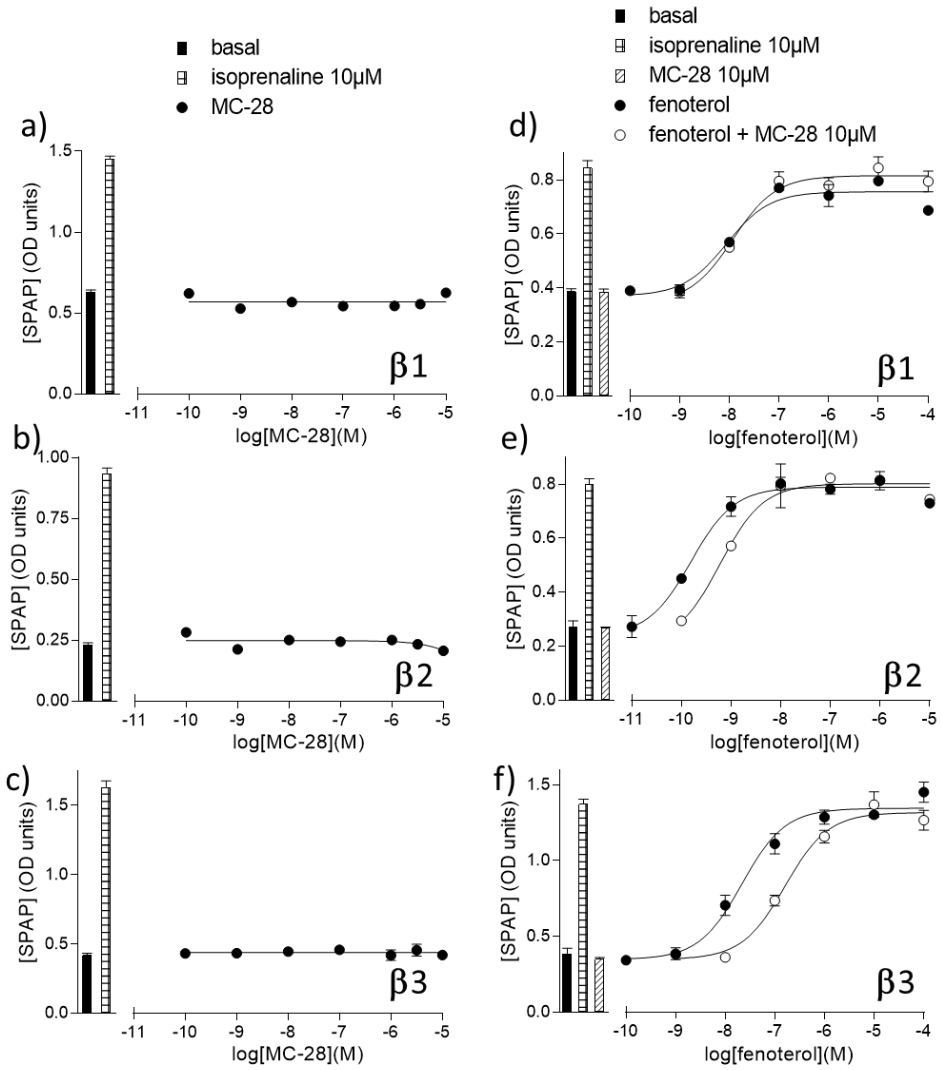

Figure 5. a–c) Concentration response curves for CRE-SPAP production by **MC28** in a) CHO-β1, b) CHO-β2 and c) CHO-β3 cells. Bars represent basal CRE-SPAP production and that in response to 10 μM isoprenaline; d–f) CRE-SPAP production in response to fenoterol in the absence and presence of 10 μM **MC28** in d) CHO-β1, e) CHO-β2 and f) CHO-β3 cells. Bars represent basal CRE-SPAP production, that in response to 10 μM isoprenaline and that in response to 10 μM **MC28** alone. Data are mean ± SEM of triplicate values and are representative of a) 3, b) 3, c) 3, d) 4, e) 5 and f) 5 separate experiments.

2.4 Structure-Activity Relationships

For most of the compounds described herein our docking results predicted higher affinity scores for the inactive state of β-ARs, suggesting higher potential for inverse agonistic or antagonistic activity (Table S1). Considering the limitations of empirical-based scoring functions to reproduce the free energy of binding, especially in cases where more complex receptor activation mechanisms take place, we focused our attention in describing structure-activity observations that might aid the design of more potent β-ARs ligands.

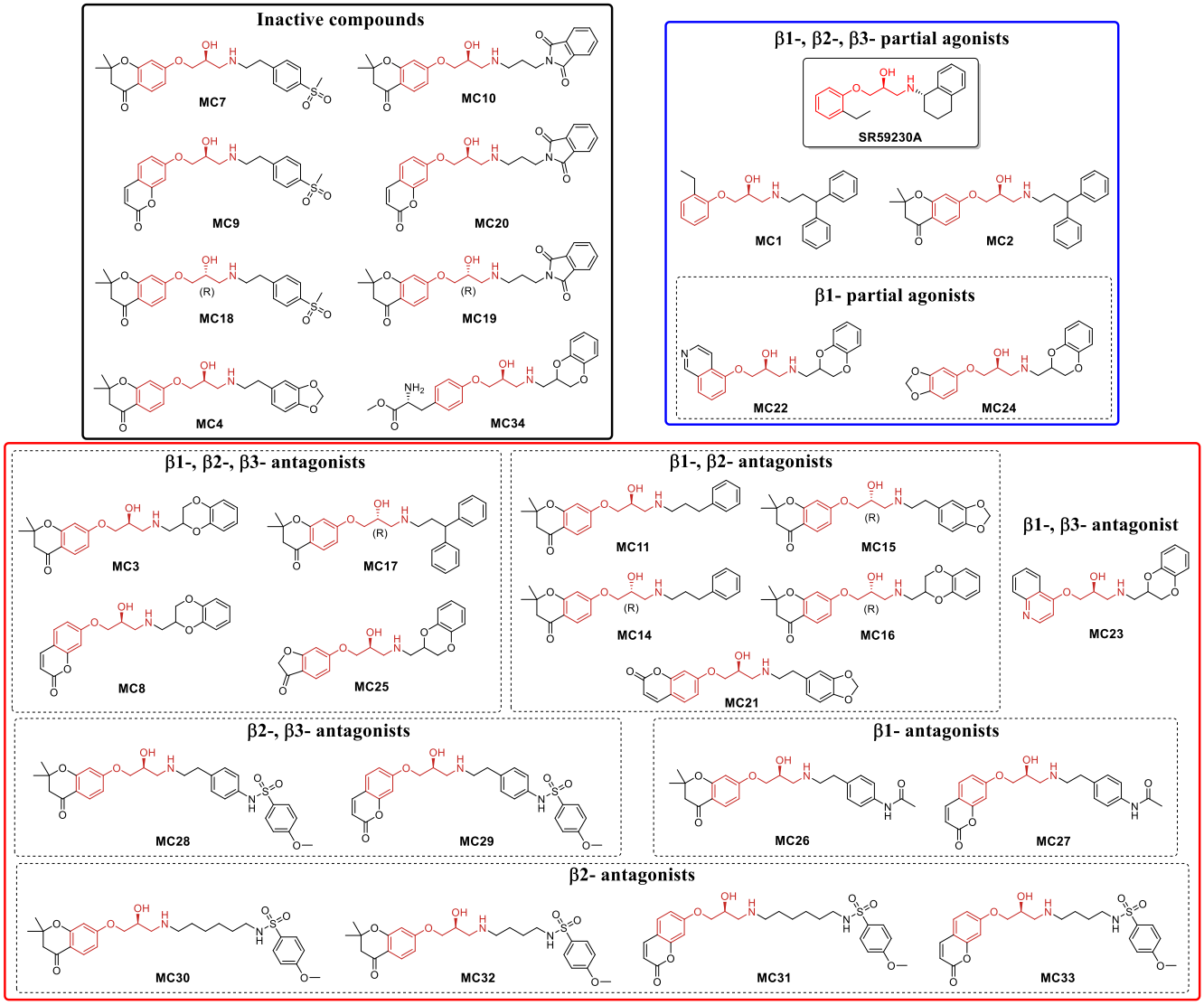

Figure 6. MC compounds grouped according to their pharmacological profile.

Pharmacological evaluations revealed **MC1** and **MC2** (Figure 6) as β-1/2/3 partial agonists (Tables 2–3). In both compounds, the R_2 group comprised a 3,3-diphenylpropyl group. **MC1** (Figure 6) was predicted to bind β-ARs in either active or inactive states with comparable scores as SR59260A, suggesting a potential antagonist to all β-ARs, a result that was in accordance with the experimental evaluation. The diphenylpropyl group is bulkier and more flexible than the tetralin moiety of SR59260, but was well accommodated within the orthosteric site of the receptors in either state. In all selected bound poses of **MC1**, the ethanolamine moiety was bound in a proper orientation and made hydrogen bonding interactions with $D^{3.32}$ and $N^{7.39}$ (Figure 7A–C).

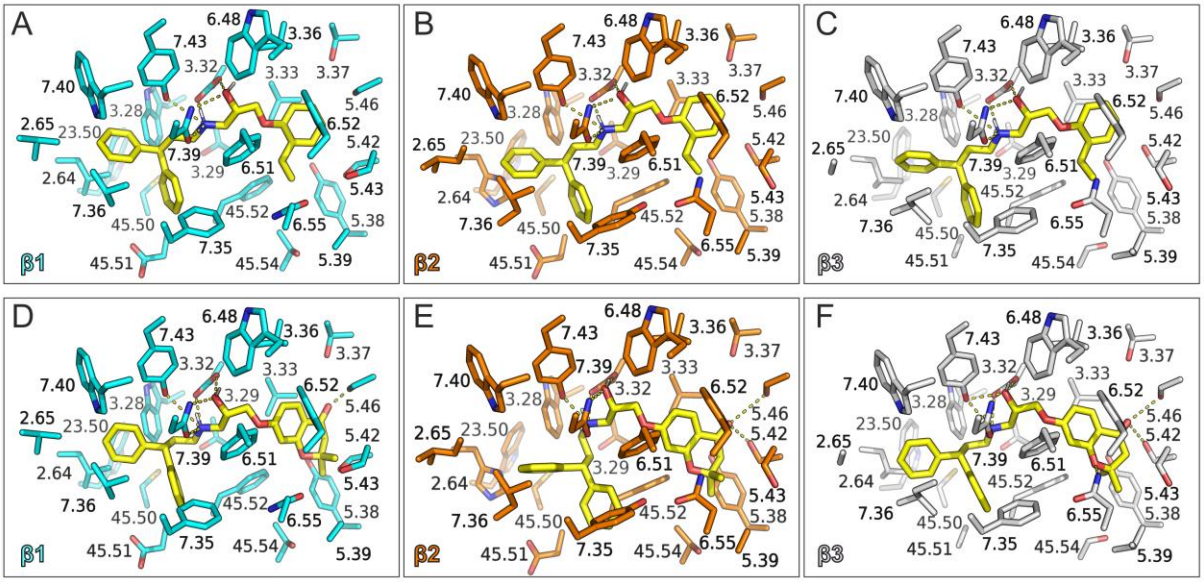

Figure 7. Predicted bound poses of **MC1** (A–C) and **MC2** (D–E) in the ligand-binding site of the three β-AR subtypes in the inactive state. Atom colors for β1-(A, D), β2-(B, E) and β3-AR (C, F) and the ligands are as in Figure 2.

MC2 (Figure 6) was found to display equally potent antagonist activity as **MC1** and SR59260A to the β-ARs, and with higher activity for β2- in comparison with β1- and β3-ARs. Our docking results indicate that substitution of the ethylbenzene group of SR59260A by 2,2-dimethylchroman-4-one (hereafter the chromanone R_1 group) resulted in potential hydrogen bonding interactions with $S^{5.42}$/$S^{5.46}$ and $N^{6.55}$ (Figure 7D–E). However, the exact rotameric state of these 3 residues and $Y^{5.38}$ within each receptor subtype can influence the exact conformation of the chromanone group though van der Waals interactions with the geminal methyl groups, and thus explains the difference for each receptor subtype. It should be noted that our docking calculations using the active states of β-ARs suggested that **MC2** cannot be accommodated properly within the orthosteric site, in particular for β2-AR, for which no docked pose was determined (Table S4). However, **MC2** displayed activity as a partial agonist of the β-ARs, suggesting that conformational changes of the receptors upon ligand binding may mediate accommodation of **MC2** in active states slightly different from the X-ray structures used in our calculations. The R-stereoisomer of **MC2**, compound **MC17** (Figure 6**,** β1-/β2-/β3-antagonist), displayed a 6- to 12-fold drop in affinity for all three β-ARs, however, this was only reflected in the binding scores of the β1-AR (Table 3). In general, most poses of the (R)-enantiomers (**MC14**–**MC19,** Figure 6) assayed did not display the proper orientation of the ethanolamine moiety in the

active state of the receptors (Table S1). The estimated scores of all the R-stereoisomers were lower than the corresponding values of their *S*-stereoisomers, indicating a lower affinity for β-ARs. However, docking in the inactive states revealed bound poses with a proper orientation of the ethanolamine moiety, except for **MC15**, **MC18** in β1-/β2-ARs, and **MC19** in β3-AR. Although of low affinity, **MC14, MC15, MC16** and **MC17** were shown to act as antagonists of β1- and β2-AR, with comparable affinity to that of their *S*-stereoisomers. This suggests that the ethanolamine moiety in the R-configuration can be accommodated in a way as to provide the key H-bonding interactions with $D^{3.32}$ and $N^{7.39}$ as illustrated by the predicted poses of **MC14** and the (S)-enantiomer **MC11** in complex with β2-AR (Figure S3).

MC3, **MC8**, **MC25** (Figure 6, β1-/β2-/β3-antagonists) and **MC24** (Figure 6, β1-/β2-/β3-antagonist and β1-partial agonist) that have the same 1,4-benzodioxane R_2 moiety and different R_1 groups (*i.e.* chromanone, coumarin, sesamol and benzofuranone) showed affinity for all receptor subtypes, albeit medium to low potency (K_D = 1.4 – 7.9 μM). Notably, the introduction of a (L)-tyrosine-like R_1 group in **MC34** (Figure 6, Inactive compounds) provided an inactive compound. In the same series, the presence of an 8-substituted quinoline R_1 group in **MC22** positively affected the β1-/β2-AR selectivity (K_D = 0.1 μM) compared to β3-AR (K_D = 1.3 μM). Whereas the introduction of a 5-substituted quinoline R_1 group in **MC23** abolished β2-AR binding (K_D > 10 μM). For this group of MC compounds one interesting observation was drawn from the docking calculations regarding the dihedral angle between the ethanolamine hydroxyl group and the oxymethylene bridge of R_1 (OH–CH–CH_2–O, indicated in Figure 8).

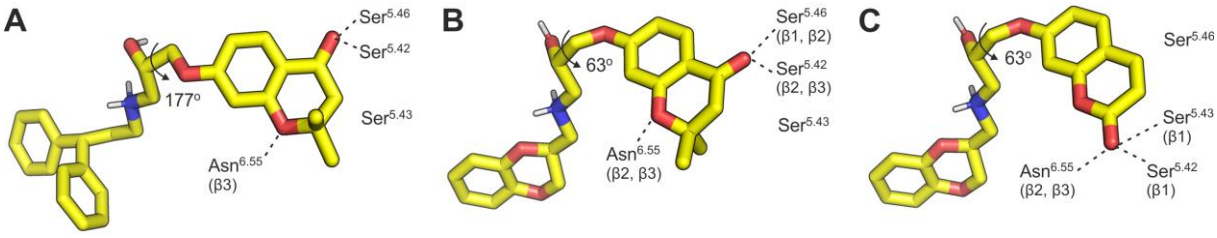

Figure 8. (A) Predicted bound pose of **MC2** in β1-AR, with hydrogen-bonding interactions of the chromenone ring indicated. The dihedral angle value between the planes of the oxymethyl bridge and the ethanolamine moiety is indicated (B) The corresponding pose for **MC3** (S,S) showing the potential H-bonding interactions with all β-ARs. (C) The corresponding conformation of **MC8** (S,S) in β1-AR.

The crystallographic structures of the most potent inverse agonists and antagonists comprising this moiety (*e.g.* carazolol) displayed an almost planar conformation with values close to 180 deg. This was also the case for the docked pose of SR59260A, **MC1** and **MC2** (Figure 8A), except only for SR59260A bound to β3-AR. In contrast, compounds **MC3** and **MC8** display an alternative conformation with a torsion around 60–80 deg (Table S4), an effect that can be ascribed to steric clashes due to the combined size of the R_1/R_2 aryl groups.

As a representative example, the chromenone group of **MC3** displayed a hydrogen bond with $S^{5.46}$ and a T-shaped aromatic interaction with $F^{6.52}$. In β2 and β3-AR, the existence of different rotameric states of $S^{5.46}$, $S^{5.42}$ and $N^{6.55}$ may accommodate **MC3** in a slightly different orientation to provide additional hydrogen-bonding interactions (Figure 8B). For **MC8** the coumarinic group is predicted to bind in a similar way as the chromenone group of **MC3**, with their aromatic rings and the endocyclic oxygen almost superimposed. However, these similar conformations give rise to different interactions with either TM5 or TM6 residues in each receptor. For β1-AR hydrogen-bonding interactions with $S^{5.42}$ and $S^{5.43}$ were predicted, whereas in β2- and β3-AR a hydrogen bond with the side-chain of $N^{6.55}$ is favored (Figure 8C). In all cases, however, a conserved T-shaped aromatic interaction with $F^{6.52}$ is displayed. Although these observations cannot be regarded as a general rule, most of the least active compounds displayed either no proper hydrogen bonding pattern to the ethanolamine moiety with the conserved $D^{3.32}$ and $N^{7.39}$, or were accommodated with a dihedral angle (OH–CH–CH_2–O) of 60–80 deg, instead of 160–180 deg. Similar observations have been drawn in previous computational studies of β-AR agonists and antagonists[77,78].

With regard to the conformation of the R_2 substituent, subtle conformational differences in the three receptors gave rise to different predicted poses, even if the R_1 substituent bound in a similar manner. For example, comparison of **MC3** in the three β-ARs revealed that the most favorable orientation of the 1,4-benzodioxane group in β2-AR is different from the β1- and β3-AR bound poses (Figure S4), an effect that can be attributed to the non-conserved residues at positions 7.35, 7.36 and 2.64. This observation contrasts with the predicted poses of **MC8,** which display the same orientation of the 1,4-benzodioxane group in all receptors and similar interactions with residues 2.64, 2.65 and 7.36 in addition to an aromatic interaction with the conserved $W^{3.28}$. Considering that **MC3** and **MC8** displayed a similar pharmacological profile

(Table 3), it can be assumed that the subtle differences in the conformation of the 1,4-benzodioxane R_2 group between receptor subtypes does not affect their response.

Comparison of the docking results of **MC3** and **MC22** (Figure 6), was used to understand differences that might explain their diverse activity as partial agonists using β1-AR in the inactive and the active states (Figure S5). In either state, the 1,4-benzodioxane and ethanolamine moieties of both compounds exhibit similar interactions with TM2 and TM7 residues of β1-AR. In contrast, the R_1 substituent of the two ligands adopted a different orientation, so that the chromanone group of **MC3** accepted a hydrogen-bond from $S^{5.46}$, whereas the isoquinoline group of **MC22** accepted a hydrogen bond from $S^{5.42}$. This observed difference may account for the observed partial agonistic activity of **MC22**, considering that the interaction with $S^{5.42}$ has been identified as a critical interaction for agonists.[69]

Our docking results demonstrate that the dioxole R_1 group of **MC24** (*S, S*) is oriented properly between $S^{5.46}$ and $S^{5.42}$ and acts as hydrogen acceptor for both residues. Although subtle differences between the three AR subtypes in the inactive state were predicted to mediate different hydrogen bonding interactions (Figure S6), pharmacological evaluation of **MC24** revealed no remarkable selectivity.

In addition, compounds **MC18**, **MC19**, **MC34**, **MC4**, **MC7**, **MC9**, **MC10**, and **MC20** (Figure 6, inactive compounds) were found to be inactive (K_D > 10 μM, Table 3), and the combination of benzyl sulphonyl and phthalimide R_2 moieties with both chromanone R_1 groups (**MC7**/**MC18** and **MC10**/**MC19** respectively) and coumarin R_1 group (**MC9** and **MC20**) were not efficient. Our docking calculations for inactive compounds **MC4, MC7, MC10** (R_1=chromanone) and **MC9, MC20** (R_1=coumarin) suggest that these compounds can bind the receptors with conformations similar to those predicted for **MC3** and **MC8** (Figure 8B, C), with subtle shifts of the chromanone substituent in β3-AR to allow for an additional interaction with $S^{5.46}$. In contrast, their pharmacological evaluation revealed that neither of these compounds exerts antagonistic activity to any of the β-AR, which agrees with their binding mode that imposes a OH–CH–CH_2–O torsion of 60–80 deg (Table S4). It should be noted that **MC4** and its (R)-enantiomer **MC15** (with the benzodioxole R_2 and chromanone R_1 groups, Figure 6) have different pharmacological profiles (Table 3). **MC4** is inactive, whereas **MC15** is a poor antagonist *vs* β1- and β2-ARs. The analog derivative **MC21** (Figure 6, β1-/β2-antagonists), with the coumarin R_1 group, and both (R)- and (S)-

enantiomers **MC11** and **MC14** maintained similar poor antagonist activity *vs* β1- and β2-ARs. In our docking calculation, compounds **MC11** and **MC21** (Figure 6, β1/β2-antagonists) were predicted to bind in a similar fashion as **MC8** and **MC3** (Figure6, β1/β2/β3-antagonists), respectively (Figure 8B,C), but in the case of **MC11** and **MC21** they displayed antagonistic activity at ~5 μM against β1- and β2-AR. Overall, these observations suggest that the exact orientation of the R_2 group is affected by subtle changes in the orientation of residues at position 2.64, 7.35 and 7.36 (Figure S7).

The introduction of benzylacetamide (**MC26–27,** Figure 6), and *p*-methoxy-benzenesulfonamide (**MC28**–**33,** Figure 6) moieties within both chromanone- and coumarin-based series, abolished the poor antagonistic activity towards one or more receptor subtypes providing MC compounds with some extent of selectivity. In particular, **MC26** and **MC27** that contain a benzylacetamide R_2 moiety displayed a degree of selectivity for β1-AR (K_D = 1.7 and 3.2 μM) *vs* β2-/β3-AR (K_D > 10 μM). Our docking results for **MC27** might provide a putative explanation for the observed activity even though this was not reflected in the binding score for each receptor. The acetamide group in R_2 of **MC27** was predicted to act as a H-bond acceptor for the indole group of $W^{7.40}$ in β1-AR, whereas the same group interacted with $D^{45.51}$ of the ECL2 in β2-AR (Figure S8). A different H-bonding interaction was also predicted for the coumarin R_1 group in **MC27**, which probably accounted for the different affinity to β1- with respect to β2- and β3-AR, for which an improper hydrogen-bonding interaction with the $D^{3.32}$ and $N^{7.39}$ was predicted. Still, it has to be emphasized that selectivity for one of the receptors is probably determined by ligand kinetics and receptor activation, rather than ligand binding modes.[27,58,79]

MC28 and **MC29** (Figure 6) contain a *p*-methoxy-benzensulfonamide R_2 group linked *via* 2 carbon atoms prefer β2- and β3-ARs (K_D = 1.2 –3.1 μM) *vs* β1-AR (K_D > 10 μM). Whereas the presence of a 4 or 6 carbon chain in compounds **MC30**–**MC33** provided selectivity for β2-AR (K_D = 0.9 – 1.6 μM) *vs* β1- and β3-ARs (K_D > 10 μM). These results indicate that a degree of selectivity can be obtained by fine-tuning the R_2 substituent within both series of chromanone- and coumarin-based compounds. In particular, the introduction of the *p*-methoxy-benzenesulfonamide group can direct selectivity against β1-AR, and that the flexibility of the aliphatic chain (**MC30–33**) instead of the benzene ring (**MC28, MC29**) mediates a higher degree of selectivity towards β2-AR. Our docking results for **MC28, MC29, MC32** and **MC33** displayed

poses with the ethanolamine moiety, while not optimally interacting with $D^{3.32}$. This suggests that the introduction of a bulky *p*-methoxy-benzenesulfonamide may affect the orientation or position of the protonated amine resulting in the loss of hydrogen bonding interactions with $D^{3.32}$. However, docking of **MC30** and **MC31** revealed conformations with a proper orientation of the ethanolamine moiety suggesting that the introduction of a long hexyl chain allows for a better accommodation of the sulfonamide group without affecting the proper orientation of the ethanolamine moiety (Figure 9). The length of the alkyl chain allows the sulfonamide group to reach an exosite and interact with residues of ECL2 (Figure 9A,B). However, this substituent is not optimal for mediating hydrogen-bonding interactions with polar $D^{45.51}$ and $K^{7.32}$. As an effect, in order to accommodate properly in β1-AR and maintain proper hydrogen-bonding interactions with $D^{3.32}$ and $N^{7.39}$, potential clashes could be introduced (Figure 9C).

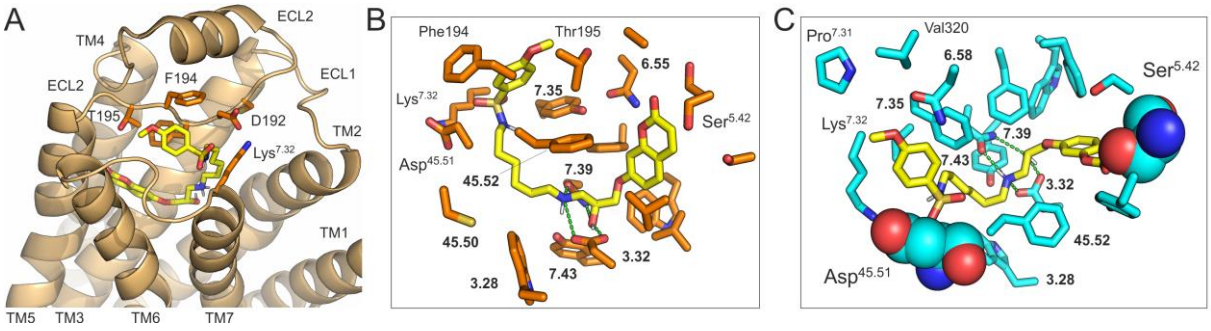

Figure 9. (A) **MC31** (yellow-C sticks) bound with the inactive state of β2-AR (orange cartoon). Interacting ECL2 residues with the benzenesulfonamide group are highlighted as orange-C sticks. (B) Close-up view of the inactive β2-AR binding pocket illustrating interacting residues within 3.5 Å of **MC31**. Key interactions with $D^{3.32}$ and $N^{7.39}$ are marked with green dashed lines. (C) Stick representation of inactive β1-AR binding pocket (cyan-C sticks) within 3.5 Å of **MC31,** illustrating the two residues that may provide van der Waals clashes with the ligand as cyan spheres.

3. Conclusions

In summary, a panel of 30 new compounds with a wide structural diversity have been designed and synthesized. The assessment of their pharmacological profile combined with extensive and comparative docking calculations *vs* all the three β-AR subtypes enabled us to identify the key molecular entities that ensured higher affinity and selectivity. Indeed, our findings support the previously reported data showing that **SR59230A** is clearly not a β3-AR selective ligand, and it shows a β1-/β2-/β3-partial agonism. From the compounds presented here, **MC28** is the most selective β3 blocker

and **MC30**–**33** are β2-selective antagonists. Notably, neither of these compounds displayed any agonist activity. Therefore, we have identified new lead compounds which can pave the ground for further development of selective and high-affinity β-AR blockers. We anticipate that such compounds will be invaluable tools in pharmacological studies of β-ARs within different cancer settings.

Acknowledgment

B.R. and J.T. thank L'Amore di Matteo Coveri ONLUS for financial support. B.R. and U.G. and the Banca d'Italia (grant prot. N° 01543393/22) for financial support. B.R., J.T. and J.B. thank the COST Action ERNEST CA18133. L.L was supported by an Erasmus+ Mobility 2020/2021 fellowship and V.N. was supported by a fellowship from Fondazione Umberto Veronesi. U.C. acknowledges the financial support from Associazione Italiana Ricerca sul Cancro (grant IG-21320), Italian Ministry of Health (grant RF-2016-02362551). The work in U.C.'s lab was partially supported by the Italian Ministry of Health with Ricerca Corrente and 5x1000 funds.

Abbreviations

GPCRs: G-protein-coupled receptors

β-ARs: β-adrenergic receptors

ECL: extracellular loop

TM: transmembrane

CHO: Chinese hamster ovary

CGP20712A: 2-hydroxy-5-(2-[{hydroxy-3-(4-[1-methyl-4-trifluoromethyl-2-imidazolyl]phenoxy)propyl}amino]ethoxy)benzamide

CRE-SPAP: cAMP response element - secreted placental alkaline phosphate

cAMP: Cyclic Adenosine Monophosphate

ICI118551: (−)-1-(2,3-[dihydro-7-methyl-1H-inden-4-yl]oxy)-3-([1-methylethyl]-amino)-2-butanol

SR59230A: 1-(2-ethylphenoxy)-3-[[(1S)-1,2,3,4-tetrahydro-1-naphthalenyl]amino]-(2S)-2-propanol

4. Experimental

4.1 Material and Methods

All reagents were purchased from Sigma-Aldrich and they have been used without any further purification, unless specified otherwise. L748,337 was purchased from Tocris Bioscience and used without any further purification. SR59230A was synthesized starting from commercially available reagents (**Scheme S7**). NMR spectra were recorded on Varian Inova 400, Mercury plus 400 and Gemini 200 instruments. ESI-MS

were recorded on LC-MS LCQ Fleet ThermoFisher Scientific. ESI-MS were recorded on LC-MS LCQ Fleet ThermoFisher Scientific. $[\alpha]_D$ values were measured using a JASCO DIP-370 instrument. CGP20712A (1024) was from Tocris Cookson (Avonmounth, Bristol, UK). ICI118551 (I127) and fenoterol (F1016) were from Sigma Aldrich (Poole, UK). Foetal calf serum was from PAA laboratories (Teddington, Middlesex, UK). All other reagents were from Sigma Aldrich (Poole, UK).

4.2 Computational Methods

Ensembles of conformers for each compound were generated from SMILES notations using OMEGA v3.1.[67] We used a "dense" set of parameters for the generation of up to 20,000 conformers within an energy window of 15 kcal/mol and a minimum cutoff for duplicate conformer removal (rms) of 0.3 Å. The *mmff94smod_NoEstat* force field was used for model construction and the *mmff94s_Sheff* was selected for calculation of the conformers energy.[68] Docking was performed using FRED v3.3[65] with high resolution (1.0 Å step for translation and rotation) and the Chemgauss4 scoring function.[66] The 10 top-scored poses were evaluated for residue-specific interactions using VIDA v4.4 (OpenEye Scientific, Inc) and figures were generated using PyMOL v2.3 (open-source build, Schrodinger LLC).

4.3 CRE-SPAP production

CHO-K1 (RIDD: CVCL_0214) stably expressing human β1, β2 or β3-adrenoceptors and a CRE-SPAP reporter gene were used (CHO-β1, CHO-β2 and CHO-β3)[27] and CRE-SPAP production measured as in ref[80]. Cells were grown to confluence in 100µl media (Dulbecco's modified Eagle's medium nutrient mix F12 (DMEM/F12) containing 10% fetal calf serum (FCS) and 2mM L-glutamine) in a 37°C humidified 5% CO_2: 95% air atmosphere in clear, sterile, tissue culture treated 96-well plates. 24-hours before experimentation, the cells were then serum starved by removing the media and adding 100µl serum-free media (sfm) per well. The following day, the sfm was removed from each well, and 100µl sfm or 100µl sfm containing an antagonist at the final required concentration was added to each well, and the cells were incubated for 20 minutes at 37°C. Agonist in 10µl sfm was then added to each well and the plates incubated for 5 hours (37°C humidified 5% CO_2: 95% air atmosphere). After 5 hours, all drugs and media were removed from each well and 40µl sfm was added to each well. After 1 hour of further incubation at 37°C, the plates were transferred to an 65°C oven for 30 minutes to destroy endogenous phosphatases. SPAP production was then measured by the addition of 100µl 5mM p-NPP per well (in diethanolamine buffer) and read on a Dynatech MRX plate reader at 405nM.

4.4 Data analysis

A one-site sigmoidal concentration response curve was fitted to the data in Prism 7 using the following equation:

$$Response = \frac{E_{max} \times [A]}{EC_{50} + [A]}$$

where E_{max} is the maximum response, [A] is the agonist concentration and EC_{50} is the concentration of agonist that produces 50% of the maximal response.

The affinity of antagonists (K_D values) were calculated from the rightward shift of the agonist (fenoterol) concentration response curve in the presence of a fixed concentration of antagonist using the following:

$$DR = 1 + \frac{[B]}{K_D}$$

where *DR* (dose ratio) is the ratio of the agonist concentration required to stimulate an identical response in the presence and absence of a fixed concentration of antagonist [B].

For the compounds with partial agonist activity, the antagonist K_D value was calculated as per the partial agonist method of Stephenson (1956):[81]

$$K_D partial\ agonist = \frac{Y \times [P]}{1 - Y} \quad where, Y = \frac{[A_2] - [A_1]}{[A_3]}$$

where [P] in the concentration of the partial agonist, $[A_1]$ in the concentration of the agonist at the point where the fixed partial agonist causes the same response, $[A_2]$ is the concentration of agonist causing a given response above that achieved by the partial agonist and $[A_3]$ the concentration of the agonist, in the presence of the partial agonist, causing the same stimulation as $[A_2]$.

Basal CRE-SPAP production and that in response to 10 ⌈M isoprenaline were each measured in 6 wells in each plate. All data are presented as mean ± s.e.m. of triplicate–sextuplet determinations of *n* separate experiments.

4.5 Synthesis of MC derivatives: ***MC1–11*** *and* ***MC20–34****.*

Synthesis of **MC1**. To a stirred solution of **3** (368 mg, 1.74 mmol) in dry MeOH (2 mL), **10** (104 mg, 0.58 mmol) was added. The reaction mixture was stirred at 50°C for 2 h and for additional 17 h at r.t., then, it was then concentrated under reduced pressure. The crude was diluted in ethyl acetate (50 mL) and washed with H_2O (2 x 5 mL). The organic phase was anhydrificated with Na_2SO_4, filtered and concentrated. The crude was filtered on silica gel (ethyl acetate:methanol 5:1, Rf = 0.3) to give **MC1** (114 mg, 50%) as a white glassy solid. ^{1}H-NMR (400 MHz, $CDCl_3$) δ: 7.28-7.12 (m, 12H, Ph and H_B and H_D), 6.90 (at, J_{C-B} = 7.4 Hz, 1H, H_C), 6.77 (d, J_{A-B} = 8.1 Hz, 1H, H_A), 4.18-4.10 (m, 1H, H-2), 4.03 (t, J_{6-5} = 7.9 Hz, 1H, H-6), 3.98-3.86 (m, 2H, H-1), 2.94-2.90 (A part of an ABX system, J_{A-B} = 12.3 Hz, J_{A-X} = 3.6 Hz, 1H, H-3), 2.86-2.80 (B part of an ABX system, J_{B-A} = 12.3 Hz, J_{B-X} = 3.2 Hz, 1H, H-3), 2.74-2.68 (m, 2H, H-4), 2.60 (q, J = 7.6 Hz, 2H, CH_2), 2.38-2.33 (m, 2H, H-5), 1.16 (t, J = 7.5 Hz, 3H, CH_3). ^{13}C-NMR (100 MHz, $CDCl_3$) δ: 156.09, 144.13, 132.59, 128.98, 128.58, 127.70, 127.69, 126.81, 126.37, 120.99, 111.21, 70.04, 67.63, 51.74, 48.83, 48.04, 34.73, 23.24, 14.16. ESI-MS *m/z*: for $[M-H]^-$ calcd. for $C_{26}H_{30}NO_2$ 388.24, found 388.22. $[\alpha]_D^{20}$ = + 7.3 (c = 0.9, $CHCl_3$).

Synthesis of **MC2***.* To a stirred solution of **10** (80 mg, 0.38 mmol) in dry MeOH (1 mL), **1** (80 mg, 0.32 mmol) was added. The reaction mixture was stirred at r.t. for 8 h, then it was concentrated under reduced pressure. The crude was diluted in ethyl acetate (100 mL) and washed with H_2O (2 x 5 mL). The organic phase was dried with Na_2SO_4, filtered and concentrated. The crude was filtered on silica gel (ethyl acetate:methanol 5:1, Rf = 0.3) to give **MC2** (43 mg, 30%) as a white glassy solid. ^{1}H-NMR (400 MHz, $CDCl_3$) δ: 7.77 (d, J_{B-C} = 8.8 Hz, 1H, H_B), 7.31-7.09 (m, 10H, Ph), 6.49

(dd, J_{C-B} = 8.8 Hz, J_{C-A} = 2.1 Hz, 1H, H_C), 6.33 (d, J_{A-C} = 2.2 Hz, 1H, H_A), 4.17-4.08 (m, 1H, H-2), 4.01 (t, J_{6-5} = 7.8 Hz, 1H, H-6), 3.98-3.84 (m, 2H, H-1), 2.91-2.86 (A part of an ABX system ABX, J_{A-B} = 12.2 Hz, J_{A-X} = 3.4 Hz, 1H, H-3), 2.83-2.77 (m, 1H, H-3), 2.71-2.68 (m, 2H, H-4), 2.66 (s, 2H, H_X), 2.39-2.33 (m, 2H, H-5), 1.43 (s, 6H,CH_3). ^{13}C-NMR (100 MHz, $CDCl_3$) δ: 191.04, 164.92, 161.86, 143.91, 128.63, 128.30, 127.68, 127.66, 126.47, 114.44, 109.40, 101.88, 79.63, 70.17, 66.84, 51.34, 48.82, 48.56, 47.94, 34.27, 26.68. ESI-MS *m/z*: for $[M-H]^-$ calcd. for $C_{29}H_{32}NO_4$ 458.24, found 458.26. $[\alpha]_D^{20}$ = - 3.0 (c = 1, $CHCl_3$).

Synthesis of **MC3**. To a stirred solution of **11** (40 mg, 0.242 mmol) in dry MeOH (1 mL), **1** (50 mg, 0.201 mmol) was added. The reaction mixture was stirred at r.t. for 184 h, then it was concentrated under reduced pressure. The crude was filtered on silica gel (ethyl acetate:methanol 5:1, Rf = 0.25) to give **MC3** (39 mg, 50%) as a yellow solid. ^{1}H-NMR (400 MHz, $CDCl_3$:CD_3OD 99:1) δ: 7.79 (d, J_{B-C} = 8.8 Hz, 1H, H_B), 6.89-6.82 (m, 4H, Ph), 6.55 (dd, J_{C-B} = 8.8 Hz, J_{C-A} = 3.7 Hz, 1H, H_C), 6.39 (d, J_{A-C} = 2.3 Hz, 1H, H_A), 4.31-4.27 (m, 2H, H-2), 4.26-4.23 (m, 1H, H-1), 4.09-3.99 (m, 4H, H-1, H-5 and H-6), 2.97-2.88 (m, 3H, H-1 and H-3), 2.85-2.80 (B part of an ABX system, J_{B-A} = 12.2 Hz, J_{B-X} = 7.5 Hz, 1H, H-3), 2.66 (s, 2H, H_X), 1.44 (s, 6H, CH_3). ^{13}C-NMR (100 MHz, $CDCl_3$ +1% CD_3OD) δ: 128.34, 121.55, 117.22, 109.47, 101.87, 72.38, 70.53, 68.14, 66.25, 51.66, 49.82, 48.45, 26.37. ESI-MS *m/z*: for $[M-H]^-$ calcd. for $C_{23}H_{26}NO_6$ 412.18, found 412.09. $[\alpha]_D^{20}$ = + 25.7 (c = 0.9, $CHCl_3$).

Synthesis of **MC4**. To a stirred solution of **12** (40 mg, 0.242 mmol) in dry dimethylformamide (1 mL), **1** (50 mg, 0.201 mmol) was added. The reaction mixture was stirred at 40°C for 92 h, and then concentrated under reduced pressure. The crude was filtered on silica gel (ethyl acetate:methanol 5:1, Rf = 0.3) to give **MC4** (39 mg, 47%) as a yellow solid. ^{1}H-NMR (400 MHz, $CDCl_3$) δ: 7.78 (d, J_{B-C} = 8.8 Hz, 1H, H_B), 6.76-6.62 (m, 3H, Ph), 6.51 (dd, J_{C-B} = 8.8 Hz, J_{B-A} = 2.4 Hz, 1H, H_B), 6.36 (d, J_{A-C} = 2.3 Hz, 1H, H_A), 5.92 (s, 2H, CH_2), 4.11-4.02 (m, 1H, H-2), 3.99-3.97 (m, 2H, H-1), 2.96-2.84 (m, 3H, H-4 and H-3), 2.84-2.71 (m, 3H, H-5 and H-3), 2.66 (s, 2H, H_X), 1.44 (s, 6H, CH_3). ^{13}C-NMR (100 MHz, $CDCl_3$) δ: 191.05, 165.12, 161.87, 147.74, 146.04, 133.07, 128.27, 121.54, 114.36, 109.46, 108.99, 108.30, 101.84, 100.85, 79.60, 70.60, 67.60, 51.32, 50.97, 48.55, 35.74, 26.67. ESI-MS *m/z*: for $[M-H]^-$ calcd. for $C_{23}H_{26}NO_6$ 412.18, found 412.21. $[\alpha]_D^{20}$ = + 22.4 (c = 1, $CHCl_3$).

Synthesis of **MC7**. To a stirred solution of **13** (57 mg, 0.242 mmol) in dry MeOH (1 mL), NMM (25.4 mg, 28 µL, 0.251 mmol) was added. The reaction mixture was stirred at r.t. for 10 min, then **1** (50 mg, 0.201 mmol) was added and the reaction mixture was stirred at 40°C for 48 h. The reaction mixture was concentrated under reduced pressure, then the crude was filtered on silica gel (ethyl acetate:methanol 5:1, Rf = 0.3) to give **MC7** (26 mg, 27%) as a white solid. ^{1}H-NMR (400 MHz, $CDCl_3$) δ: 7.86 (d, J_{E-D} = 8.2 Hz, 2H, H_E), 7.77 (d, J_{B-C} = 8.8 Hz, 1H, H_B), 7.41 (d, J_{D-E} = 8.2 Hz, 2H, H_D), 6.52 (dd, J_{C-B} = 8.8 Hz, J_{C-A} = 2.4 Hz, 1H, H_C), 6.36 (d, J_{A-C} = 2.3 Hz, 1H, H_A), 4.10-4.03 (m, 1H, H-2), 3.97 (d, J = 4.9 Hz, 2H, H-1), 3.04 (s, 3H, S-CH_3), 3.01-2.93 (m, 4H, H-4 and H-5), 2.92-2.87 (A part of an ABX system, J_{A-B} = 12.3 Hz, J_{A-X} = 3.8 Hz, 1H, H-3), 2.82-2.77 (B part of an ABX system, J_{B-A} = 12.2 Hz, J_{B-X} = 8.1 Hz, 1H, H-3), 2.66 (s, 2H, H_X), 1.43 (s, 6H, CH_3). ^{13}C-NMR (100 MHz, $CDCl_3$) δ: 191.17, 165.00, 161.87, 129.70, 128.34, 127.69, 110.49, 109.42, 101.78, 79.71, 70.42, 67.70, 51.30, 50.35, 48.50, 44.55, 36.11, 26.68. ESI-MS *m/z*: for $[M-H]^+$ calcd. for $C_{23}H_{29}NO_6S$ 446.17, found 446.15. $[\alpha]_D^{20}$ = + 41.1 (c = 0.8, $CHCl_3$).

Synthesis of **MC8**. To a stirred solution of **11** (36 mg, 0.220 mmol) in dry MeOH (1 mL), **2** (40 mg, 0.183 mmol) was added. The reaction mixture was stirred at 40°C for

72 h, and then concentrated. The crude was filtered on silica gel (ethyl acetate:methanol 5:1, Rf = 0.35) to give **MC8** (30 mg, 43%) as a white solid. ^{1}H-NMR (400 MHz, $CDCl_3$) δ: 7.63 (d, J_{D-E} = 9.5 Hz, 1H, H_D), 7.37 (d, J_{C-A} = 8.5 Hz, 1H, H_C), 6.92-6.79 (m, 6H, H_A, H_B and Ph), 6.26 (d, J_{E-D} = 9.5 Hz, 1H, H_E), 4.35-4.30 (m, 1H, H-2), 4.29-4.25 (A part of an ABX system, J_{A-B} = 11.3 Hz, J_{A-X} = 2.2 Hz, 1H, H-6), 4.14-4.08 (m, 1H, H-5), 4.07-4.05 (m, 2H, H-1), 4.04-4.01 (B part of an ABX system, J_{B-A} = 11.3 Hz, J_{B-X} = 2.3 Hz, 1H, H-6), 3.03-2.99 (A part of an ABX system, J_{A-B} = 11.1 Hz, J_{A-X} = 5.2 Hz, 1H, H-3), 2.99-2.94 (m, 2H, H-4), 2.88-2.83 (B part of an ABX system, J_{B-A} = 12.3 Hz, J_{B-X} = 7.7 Hz, 1H, H-3). ^{13}C-NMR (100 MHz, $CDCl_3$) δ: 143.23, 128.71, 121.43, 117.15, 113.24, 112.68, 101.58, 72.28, 70.75, 68.00, 66.18, 51.56, 49.71. ESI-MS *m/z*: for $[M-H]^+$ calcd. for $C_{21}H_{20}NO_6$ 384.14, found 384.10. $[\alpha]_D^{20}$ = + 23.3 (c = 1, $CHCl_3$).

Synthesis of **MC9**. To a suspension of **13** (67 mg, 0.284 mmol) in *2*-propanol (1 mL), DIPEA (55 µL, 0.312 mmol) was added. After 20 min at r.t., a solution of compound **2** (31 mg, 0.142 mmol) in a mixture *2*-propanol: MeOH 2:1 (1.5 mL) was added and the reaction mixture was stirred at 30°C for 48 h. Then, the reaction mixture was concentrated under reduced pressure. The crude was filtered on silica gel (dichloromethane:methanol 10:1, Rf = 0.2) to give **MC9** (42 mg, 65%) as a yellow oil. ^{1}H-NMR (400 MHz, DMSO-d^6) δ: 7.99 (d, J_{D-E} = 9.5 Hz, 1H, H_D), 7.88 (d, J_{G-F} = 8.4 Hz, 2H, H_G), 7.64 (d, J_{C-A} = 8.7 Hz, 1H, H_C), 7.54 (d, J_{F-G} = 8.3 Hz, 2H, H_F), 7.01 (d, J_{B-A} = 2.4 Hz, 1H, H_B), 6.96 (dd, J_{A-C} = 8.6 Hz, J_{A-B} = 2.4 Hz, 1H, H_A), 6.29 (d, J_{E-D} = 9.5 Hz, 1H, H_E), 5.94 (s, 1H, H_N), 4.24-4.21 (m, 1H, H-2), 4.16-4.03 (m, 2H, H-1), 3.23-3.19 (m, 2H, H-4), 3.18 (s, 3H, CH_3), 3.16-3.15 (m, 1H, H-3), 3.12-3.05 (m, 2H, H-5), 3.02 (B part of an ABX system, J_{B-A} = 12.6 Hz, J_{B-X} = 9.5 Hz, 1H, H-3). ^{13}C-NMR (100 MHz, DMSO-d^6) δ: 144.48, 130.36, 130.28, 127.97, 113.39, 113.00, 101.51, 70.72, 65.12, 49.80, 47.94, 43.92, 31.75. ESI-MS *m/z*: for $[M-H]^+$ calcd. for $C_{21}H_{22}NO_6S$ 416.12, found 416.09. $[\alpha]_D^{20}$ = + 49.2 (c = 0.9, $CHCl_3$).

Synthesis of **MC10**. To a strirred solution of **14** (97 mg, 0.40 mmol) in 2-propanol (1 mL), DIPEA (78 µL, 0.44 mmol) was added. The solution was stirred at r.t. for 30 min, then **1** (50 mg, 0.2 mmol) was added. The reaction mixture was stirred at r.t. for 96 h, then it was concentrated under reduced pressure. the crude was filtered on silica gel (dichloromethane:methanol 10:1, Rf = 0.4) to give **MC10** (11 mg, 12%) as a white solid. ^{1}H-NMR (400 MHz, $CDCl_3$ +5% CD_3OD) δ: 7.81-7.67 (m, 4H, Phth), 7.52-7.49 (m, 1H, H_B), 6.52 (dd, J_{C-B} = 8.7 Hz, J_{C-A} = 1.9 Hz, 1H, H_C), 6.38 (d, J_{A-C} = 1.6 Hz, 1H, H_A), 4.72-4.67 (m, 1H, H-2), 4.12-4.06 (m, 1H, H-1), 4.06-4.02 (m, 3H, H-1, H-6), 3.11-3.08 (m, 1H, H-3), 2.99-2.94 (m, 1H, H-3), 2.63 (s, 2H, H_X), 2.10-1.92 (m, 4H, H-5, H-4), 1.4 (s, 6H, CH_3). ^{13}C-NMR (100 MHz, $CDCl_3$ +5% CD_3OD) δ: 191.50, 168.83, 168.58, 164.49, 161.97, 134.31, 134.22, 131.70, 128.36, 123.45, 123.36, 109.30, 102.09, 79.71, 69.75, 37.22, 34.59, 26.70, 26.56. ESI-MS *m/z*: for $[M-H]^+$ calcd. for $C_{25}H_{28}N_2O_6$ 451.19, found 451.15. $[\alpha]_D^{20}$ = + 5.6 (c = 0.7, $CHCl_3$).

Synthesis of **MC11**. To a stirred solution of **15** (26 mg, 0.199 mmol) in dry 2-propanol (1 mL), **1** (33 mg, 0.133 mmol) was added. The reaction mixture was stirred at r.t. for 48 h. After this, the reaction mixture was evaporated under reduced pressure. The crude was filtered through silica gel (ethyl acetate:methanol 5:1, Rf = 0.3) to give **MC11** (48 mg, 94%) as a white solid. ^{1}H-NMR (400 MHz, $CDCl_3$) δ: 7.78 (d, J_{B-C} = 8.8 Hz, 1H, H_B), 7.29-7.27 (m, 2H, Ph), 7.20-7.16 (m, 3H, Ph), 6.53 (dd, J_{C-B} = 8.8 Hz, J_{C-A} = 1.9 Hz, 1H, H_c), 6.36 (d, J_{A-C} = 2.0 Hz, 1H, H_A), 4.19-4.10 (m, 1H, H-2), 4.04-4.01 (m, 2H, H-1), 2.99-2.88 (m, 1H, H-3), 2.84-2.77 (m, 3H, H-3 e H-4), 2.75-2.71 (m, 4H, H_X e H-5), 2.01-1.89 (m, 2H, H-6), 1.50 (s, 6H, CH_3). ^{13}C-NMR (100 MHz, $CDCl_3$) δ:

161.96, 128.47, 128.35, 126.09, 109.5, 101.94, 70.61, 67.43, 51.59, 49.06, 48.58, 30.81, 26.70**.** ESI-MS *m/z*: for $[M-H]^+$ calcd. for $C_{23}H_{28}NO_4$ 382.21, found 382.16. $[\alpha]_D^{20}$ = + 59.7 (c = 1, $CHCl_3$).

Synthesis of **MC20**. To a stirred solution of **14** (30 mg, 0.124 mmol) in 2-propanol (1 mL), DIPEA (24 µL, 0.136 mmol) was added. The solution was stirred at r.t. for 30 min, then **2** (15 mg, 0.065 mmol) was added. The reaction mixture was stirred at r.t. for 144 h, and then was concentrated under reduced pressure. The crude was filtered on silica gel (ethyl acetate:methanol 5:1, Rf = 0.2) to give **MC20** (10 mg, 37%) as a white solid. ^{1}H-NMR (400 MHz, DMSO-d^6) δ: 7.97 (d, J_{D-E} = 9.5 Hz, 1H, H_D), 7.86-7.80 (m, 4H, Phth), 7.61 (d, J_{B-A} = 8.5 Hz, 1H, H_B), 6.96-6.92 (m, 2H, H_A, H_C), 6.27 (d, J_{E-D} = 9.5 Hz, 1H, H_E), 4.09-4.04 (m, 1H, H-2), 3.99-3.93 (m, 2H, H-1), 3.68-3.60 (m, 2H, H-6), 3.23-3.17 (m, 1H, H-3), 2.82-2.76 (m, 1H, H-3), 2.71-2.66 (m, 2H H-4), 1.86-1.65 (m, 4H, H-4, H-5). ^{13}C-NMR (50 MHz, DMSO-d^6) δ: 168.56, 168.52, 168.44, 162.21, 160.73, 155.78, 144.78, 136.82, 136.15, 134.80, 132.12, 129.93, 129.75, 128.03, 123.44, 113.20, 112.94, 112.82, 101.71, 71.55, 37.57, 37.29, 37.08, 35.93, 29.44, 28.47. ESI-MS *m/z*: for $[M-H]^+$ calcd. for $C_{23}H_{21}N_2O_6$ 421.15, found 421.12. $[\alpha]_D^{20}$ = + 14.3 (*c* = 1, $CHCl_3$).

Synthesis of **MC21**. To a stirred solution of **12** (61 µL, 0.443 mmol) in 2-propanol (1 mL), **2** (44 mg, 0.201 mmol) was added. The reaction mixture was stirred at r.t. for 93 h, then it was concentrated under reduced pressure. The crude was filtered on silica gel (ethyl acetate:methanol 5:1, Rf = 0.2) to give **MC 21** (60 mg, 78%) as a white solid. ^{1}H-NMR (400 MHz, $CDCl_3$ +5% CD_3OD) δ: 7.61 (d, J_{D-E} = 9.5 Hz, 1H, H_D), 7.32 (d, J_{B-A} = 8.6 Hz, 1H, H_B), 6.78 (dd, J_{A-B} = 8.6 Hz, J_{A-C} = 2.3 Hz, 1H, H_A), 6.74 (d, J_{C-A} = 2.3 Hz, 1H, H_C), 6.67-6.57 (m, 3H, Ph), 6.18 (d, J_{E-D} = 9.5 Hz, 1H, H_E), 5.84 (s, 2H, CH_2), 4.13-4.05 (m, 1H, H-2), 3.95-3.90 (m, 2H, H-1), 2.92-2.81 (m, 3H, H-4 and H-3), 2.81-2.70 (m, 3H, H-5 and H-3). ^{13}C-NMR (100 MHz, $CDCl_3$ +5% CD_3OD) δ: 161.85, 161.65, 155.65, 147.80, 146.19, 143.72, 132.35, 128.89, 121.53, 113.00, 112.84, 108.91, 108.33, 101.68, 100.86, 70.85, 67.27, 51.40, 50.67, 34.78. ESI-MS *m/z*: for $[M-H]^+$ calcd. for $C_{21}H_{20}NO_6$ 384.14, found 384.11. $[\alpha]_D^{20}$ = + 39.9 (*c* = 0.8, $CHCl_3$).

Synthesis of **MC22**. To a stirred solution of **11** (51 mg, 0.31 mmol) in 2-propanol (0.7 mL), **5** (31 mg, 0.15 mmol) was added. The reaction mixture was stirred at r.t for 89 h, then it was concentrated under reduced pressure. The crude was purified by filtration on silica gel (ethyl acetate:methanol 12:1, Rf = 0.1) to give **MC22** (15 mg, 28%) as a red oil. ^{1}H-NMR (400 MHz, CD_3OD) δ: 9.14 (s, 1H, H_D), 8.37 (d, J_{F-E} = 5.9 Hz, 1H, H_F), 8.15 (d, J_{E-F} = 5.9 Hz, 1H, H_E), 7.63-7.55 (m, 2H, H_B and H_C), 7.19 (d, J_{A-B} = 7.5 Hz, 1H, H_A), 6.81-6.75 (m, 4H, H-7 and H-8), 4.29-4.18 (m, 5H, H-1, H-2, H-5 and H-6), 3.98-3.93 (B part of an ABX system, J_{B-A} = 11.6 Hz, J_{B-X} = 7.6 Hz, 1H, H-1), 3.01-2.89 (m, 4H, H-3 and H-4). ^{13}C-NMR (100 MHz, CD_3OD) δ: 153.48, 151.06, 143.30, 142.96, 140.93, 129.53, 128.53, 127.91, 121.04, 120.96, 119.28, 116.83, 116.58, 115.48, 109.27, 72.51, 70.84, 68.36, 66.08, 51.98, 49.34. ESI-MS *m/z*: for $[M-H]^+$ calcd. for $C_{21}H_{21}N_2O_4$ 365.16, found 365.15. $[\alpha]_D^{20}$ = + 1.5 (*c* = 1, $CHCl_3$).

Synthesis of **MC23**. To a stirred solution of **11** (82 mg, 0.49 mmol) in 2-propanol (1 mL), **6** (50 mg, 0.24 mmol) was added. The reaction mixture was stirred at r.t for 89 h, and concentrated under reduced pressure. The crude was purified by filtration on silica gel (ethyl acetate:methanol 12:1, Rf = 0.2) to give **MC23** (60 mg, 68%) as a white solid. ^{1}H-NMR (400 MHz, CD_3OD) δ: 8.34 (d, *J* = 6.9 Hz, 1H, H_B), 8.02 (dd, *J* = 7.6, 2.0 Hz, 1H, H_D), 7.85 (dd, *J* = 8.9, 3.4 Hz, 1H, H_C), 7.48-7.44 (m, 1H, H_A), 6.86-6.78 (m, 4H, Ph), 6.31 (d, *J* = 7.6 Hz, 1H, H_E), 4.64-4.58 (m, 1H, H-5), 4.31-4.26 (m, 1H, H-6), 4.14-4.09 (m, 2H, H-6), 4.02-3.90 (m, 2H, H-1), 2.91-2.83 (m, 3H, H-3 and H-4), 2.78-2.72

(m, 1H, H-4). ^{13}C-NMR (100 MHz, CD_3OD) δ: 178.82, 146.19, 143.30, 140.20, 132.37, 125.73, 123.85, 121.05, 120.91, 116.84, 116.61, 116.55, 116.44, 108.12, 78.04, 74.02, 72.60, 67.88, 66.09, 65.73, 56.63, 52.60, 52.52, 49.37, 41.41. ESI-MS *m/z*: for $[M-H]^+$ calcd. for $C_{21}H_{21}N_2O_4$ 365.16, found 365.13. $[\alpha]_D^{20}$ = + 24.2 (*c* = 0.9, $CHCl_3$).

Synthesis of **MC24**.To a stirred solution of **11** (289 mg, 1.75 mmol) in 2-propanol (3 mL), **3** (170 mg, 0.87 mmol) was added. The reaction mixture was stirred at r.t for 66 h, and concentrated under reduced pressure. The crude was purified by filtration on silica gel (ethyl acetate, Rf = 0.4) to give **MC24** (208 mg, 67%) as a white solid. ^{1}H-NMR (400 MHz, DMSO-d^6) δ: 6.84 – 6.75 (m, 5H, Ph and H_C), 6.59 (d, *J* = 2.5 Hz, 1H, H_A), 6.34 (dd, J_{B-C} = 8.4 Hz, J_{B-A} = 2.3 Hz, 1H, H_B), 5.93 (s, 2H, H_D), 4.96-4.95 (m, 1H, H_N), 4.32-4.28 (A part of an ABX system, J_{A-B} = 11.4 Hz, J_{A-X} = 2.3 Hz, 1H, H-1), 4.22-4.17 (m, 1H, H-2), 3.98-3.93 (B part of an ABX system, J_{B-A} = 11.4 Hz, J_{B-X} = 7.4 Hz, 1H, H-1), 3.86-3.76 (m, 3H, H-5 and H-6), 2.84-2.74 (m, 2H, H-3), 2.74-2.71 (m, 1H, H-4), 2.61-2.57 (B part of an ABX system, J_{B-A} = 11.8 Hz, J_{B-X} = 5.4 Hz, 1H, H-4). ^{13}C-NMR (100 MHz, DMSO-d^6) δ: 154.60, 148.31, 143.55, 143.51, 141.47, 121.71, 121.47, 117.48, 117.28, 108.43, 106.19, 101.37, 98.28, 73.05, 71.93, 68.56, 66.51, 53.00, 49.81. ESI-MS *m/z*: for $[M-H]^+$ calcd. for $C_{19}H_{20}NO_6$ 358.14, found 358.15. $[\alpha]_D^{20}$ = + 88.17 (*c* = 1, $CHCl_3$).

Synthesis of **MC25**.To a stirred solution of **11** (37 mg, 0.22 mmol) in 2-propanol (1 mL), **4** (24 mg, 0.11 mmol) was added. The reaction mixture was stirred at r.t for 66 h, then concentrated under reduced pressure. The crude was purified by filtration on silica gel (ethyl acetate, Rf = 0.35) to give **MC25** (18 mg, 45%) as a white solid. ^{1}H-NMR (400 MHz, $CDCl_3$) δ: 7.53 (d, J_{C-B} = 8.5 Hz, 1H, H_C), 6.84-6.77 (m, 4H, Ph), 6.74-6.70 (m, 2H, H_A and H_B), 4.30-4.27 (m, 2H, H-5 and H-1), 4.12-4.05 (m, 5H, H-1, H-2 and H_D), 3.99-3.93 (m, 1H, H-6), 2.96-2.87 (m, 3H, H-3 and H-4), 2.85-2.79 (m, 1H, H-3). ^{13}C-NMR (100 MHz, $CDCl_3$) δ: 176.92, 171.56, 167.85, 143.27, 124.44, 121.08, 120.99, 116.86, 116.61, 111.81, 96.71, 72.40, 71.10, 68.19, 66.03, 60.12, 51.60, 49.15. ESI-MS *m/z*: for $[M-H]^+$ calcd. for $C_{20}H_{20}NO_6$ 370.14, found 370.11. $[\alpha]_D^{20}$ = + 32.9 (*c* = 0.9, $CHCl_3$).

Synthesis of **MC26**.To a stirred solution of **16** (47 mg, 0.16 mmol) in 2-propanol (1 mL), triethylamine (23 µL, 0.16 mmol) was added. After 15 min, **1** (20 mg, 0.08 mmol) was added and the reaction mixture was stirred at r.t. for 89 h. Then, it was concentrated under reduced pressure. The crude was filtered on silica gel (ethyl acetate:methanol 5:1, Rf = 0.1) to give **MC26** (31 mg, 91%) as a yellow oil. ^{1}H-NMR (400 MHz, CD_3OD) δ: 7.73 (d, J_{B-C} = 8.8 Hz, 1H, H_B), 7.50 (d, *J* = 8.5 Hz, 2H), 7.22 (d, *J* = 8.5 Hz, 2H), 6.59 (dd, J_{C-B} = 8.8 Hz, J_{C-A} = 2.4 Hz, 1H, H_C), 6.47 (d, J_{A-C} = 2.3 Hz, 1H, H_A), 4.26-4.20 (m, 1H, H-2), 4.06-4.04 (m, 2H, H-1), 3.23-3.18 (m, 3H, H_D, H-3), 3.12-3.06 (B part of an ABX system, J_{B-A} = 12.6 Hz, J_{B-X} = 9.3 Hz, 1H, H-3), 2.98-2.94 (m, 2H, H_C), 2.69 (s, 2H, H_X), 2.11 (s, 3H, $COCH_3$) 1.42 (s, 6H, CH_3). ^{13}C-NMR (100 MHz, CD_3OD) δ: 192.16, 170.28, 165.44, 162.25, 137.41, 132.62, 128.68, 127.65, 120.24, 118.21, 115.30, 114.06, 109.16, 101.76, 79.41, 70.02, 65.57, 50.02, 49.14, 31.80, 25.31, 22.37. ESI-MS *m/z*: for $[M-H]^+$ calcd. for $C_{24}H_{29}N_2O_5$ 425.22, found 425.19. $[\alpha]_D^{20}$ = + 78.8 (*c* = 1, $CHCl_3$).

Synthesis of **MC27**.To a stirred solution of **16** (68 mg, 0.22 mmol) in 2-propanol (1 mL) and DMSO (200 µL), triethylamine (32 µL, 0.22 mmol) was added. After 15 min, **2** (25 mg, 0.11 mmol) was added. The reaction mixture was stirred at r.t. for 137 h, then it was concentrated under reduced pressure. The crude was filtered on silica gel (ethyl acetate:methanol 5:1, Rf = 0.1) to give **MC27** (23 mg, 53%) as a yellow oil. ^{1}H-NMR (400 MHz, CD_3OD) δ: 7.89 (d, J_{D-E} = 9.5 Hz, 1H, H_D), 7.55 (d, J_{C-A} = 8.6 Hz, 1H, H_C),

7.51 (d, $J_{G\text{-}F}$ = 8.5 Hz, 2H, H_G), 7.23 (d, $J_{F\text{-}G}$ = 8.5 Hz, 2H, H_F), 6.97 (dd, $J_{A\text{-}C}$ = 8.6 Hz, $J_{A\text{-}B}$ = 2.4 Hz, 1H, H_A), 6.93 (d, $J_{B\text{-}A}$ = 2.3 Hz, 1H, H_B), 6.26 (d, $J_{E\text{-}D}$ = 9.5 Hz, 1H, H_E), 4.64 (bs, 1H, H_N), 4.30-4.24 (m, 1H, H-2), 4.10-4.09 (m, 2H, H-1), 3.27-3.23 (m, 3H, H-4 and H-3), 3.18-3.13 (B part of an ABX system, $J_{B\text{-}A}$ = 12.6 Hz, $J_{B\text{-}X}$ = 9.5 Hz, 1H, H-3'), 3.00-2.96 (m, 2H, H-5), 2.10 (s, 3H, CH_3). ^{13}C-NMR (100 MHz, CD_3OD) δ: 170.26, 161.83, 161.78, 155.57, 144.24, 137.53, 132.27, 129.16, 128.69, 120.26, 113.07, 112.35, 101.16, 70.23, 65.32, 49.84, 48.94, 31.49, 22.35. ESI-MS *m/z*: for $[M\text{-}H]^+$ calcd. for $C_{22}H_{23}N_2O_5$ 395.17, found 395.13. $[\alpha]_D^{20}$ = + 81.2 (*c* = 1.1, $CHCl_3$).

Synthesis of **MC28**.To a stirred solution of **17** (68 mg, 0.16 mmol), in 2-propanol (1 mL), triethylamine (23 µL, 0.16 mmol) was added. After 15 min **1** (20 mg, 0.08 mmol) was added. The reaction mixture was stirred at r.t. for 138 h, and then concentrated under reduced pressure. The crude was filtered on silica gel (ethyl acetate:methanol 5:1, Rf = 0.1) to give **MC28** (23 mg, 64%) as a white solid. ^{1}H-NMR (400 MHz, CD_3OD) δ: 7.73 (d, $J_{B\text{-}A}$ = 8.8 Hz, 1H, H_B), 7.67 (d, $J_{F\text{-}G}$ = 9.0 Hz, 2H, H_F), 7.13 (d, $J_{E\text{-}D}$ = 8.5 Hz, 2H, H_E), 7.05 (d, $J_{D\text{-}E}$ = 8.5 Hz, 2H, H_D), 6.95 (d, $J_{G\text{-}F}$ = 8.9 Hz, 2H, H_G), 6.60 (dd, $J_{C\text{-}B}$ = 8.8 Hz, $J_{C\text{-}A}$ = 2.3 Hz, 1H, H_C), 6.47 (d, $J_{A\text{-}C}$ = 2.3 Hz, 1H, H_A), 4.29-4.19 (m, 1H, H-2), 4.03-4.04 (m, 2H, H-1), 3.81 (s, 3H, -OCH_3), 3.22-3.05 (m, 4H, H-3, H-4), 2.92-2.88 (m, 2H, H-5), 2.69 (s, 2H, H_X), 1.42 (s, 6H, CH_3). ^{13}C-NMR (100 MHz, CD_3OD) δ: 192.11, 165.39, 163.12, 162.23, 136.68, 133.15, 131.08, 129.04, 128.93, 127.68, 121.18, 113.70, 109.12, 101.77, 79.43, 69.98, 65.52, 54.74, 49.96, 48.96, 47.66, 31.63, 25.31. ESI-MS *m/z*: for $[M\text{-}H]^+$ calcd. for $C_{29}H_{33}N_2O_7S$ 553.21, found 553.24. $[\alpha]_D^{20}$ = - 10.7 (*c* = 1, $CHCl_3$).

Synthesis of **MC29**.To a stirred solution of **17** (96 mg, 0.22 mmol) in 2-propanol (1 mL) and DMSO (200 µL), triethylamine (32 µL, 0.22 mmol) was added. After 15 min, **2** (25 mg, 0.11 mmol) was added. The reaction mixture was stirred at r.t. for 160 h, and then it was concentrated under reduced pressure. The crude was purified by flash chromatography on silica gel (ethyl acetate:methanol 6:1, Rf = 0.1) to give **MC29** (40 mg, 69%). ^{1}H-NMR (400 MHz, CD_3OD) δ: 7.88 (d, $J_{D\text{-}E}$ = 9.5 Hz, 1H, H_D), 7.67-7.64 (m, 2H, H_H), 7.55 (d, *J* = 8.6 Hz, 1H, H_C), 7.13 (d, $J_{G\text{-}F}$ = 8.5 Hz, 2H, H_G), 7.05 (d, $J_{F\text{-}G}$ = 8.5 Hz, 2H, H_F), 6.97-6.92 (m, 4H, H_A, H_B, H_I), 6.26 (d, $J_{E\text{-}D}$ = 9.5 Hz, 1H, H_E), 4.24 (m, 1H, H-2), 4.09-4.07 (m, 2H, H-1), 3.80 (s, 3H, -OCH_3), 3.19-3.03 (m, 4H, H-3, H-4), 2.91-2.87 (m, 2H, H-5). ^{13}C-NMR (100 MHz, CD_3OD) δ: 163.11, 161.91, 155.58, 144.26, 136.60, 133.48, 131.10, 129.15, 129.02, 128.92, 121.19, 113.69, 113.02, 112.64, 101.11, 70.36, 65.84, 54.73, 50.14, 49.13, 31.99. ESI-MS *m/z*: for $[M\text{-}H]^+$ calcd. for $C_{27}H_{27}N_2O_7S$ 523.16, 523.11. $[\alpha]_D^{20}$ = + 51.1 (*c* = 0.7, $CHCl_3$).

Synthesis of **MC30**.To a stirred solution of **18** (97 mg, 0.24 mmol) in 2-propanol (1mL), triethylamine (50 µL, 0.36 mmol) was added. After 30 min, **1** (30 mg, 0.12 mmol) was added. The reaction mixture was stirred at r.t for 118 h, then it was concentrated under reduced pressure. The crude was purified by flash chromatography on silica gel (ethyl acetate:methanol 5:1, Rf = 0.3) to give **MC30** (16 mg, 25%) as a white solid. ^{1}H-NMR (400 MHz, $CDCl_3$) δ: 7.68-7.63 (m, 3H, H_B, H_A'), 6.89-6.85 (m, 2H, H_B'), 6.43 (dd, $J_{C\text{-}B}$ = 8.8 Hz, $J_{C\text{-}A}$ = 2.4 Hz, 1H, H_C), 6.28 (d, $J_{A\text{-}C}$ = 2.4 Hz, 1H, H_A), 4.26-4.20 (m, 1H, H-2), 3.95-3.91 (A part of an ABX system, $J_{A\text{-}B}$ = 9.8 Hz, $J_{A\text{-}X}$ = 4.9 Hz, 1H, H-1), 3.89-3.85 (B part of an ABX system, $J_{B\text{-}A}$ = 9.8 Hz, $J_{B\text{-}X}$ = 5.4 Hz, 1H, H-1), 3.75 (s, 3H, -OCH_3), 3.25-3.24 (m, 1H, H_N propanolamine), 3.06-3.02 (A part of an ABX system, $J_{A\text{-}B}$ = 12.5 Hz, $J_{A\text{-}X}$ = 3.0 Hz, 1H, H-3), 2.94-2.88 (B part of an ABX system, $J_{B\text{-}A}$ = 12.5 Hz, $J_{B\text{-}X}$ = 9.9 Hz, 1H, H-3), 2.83 (td, *J* = 7.1 Hz, *J* = 2.1 Hz, 2H, H-9), 2.73 (t, $J_{4\text{-}5}$ = 6.8 Hz, 2H, H-4), 2.55 (s, 2H, H_X), 1.62-1.56 (m, 2H, H-8), 1.38-1.35 (m, 2H, H-5), 1.33 (s, 6H, CH_3), 1.25-.122 (m, 4H, H-6, H-7). ^{13}C-NMR (100 MHz, $CDCl_3$) δ: 195.92, 168.97,

166.65, 166.03, 135.42, 132.85, 132.16, 118.20, 118.08, 113.32, 105.83, 83.59, 73.80, 69.31, 59.41, 54.41, 52.24, 52.13, 46.51, 32.79, 30.35, 29.94, 29.71, 29.60. ESI-MS *m/z*: for $[M-H]^+$ calcd. for $C_{27}H_{37}N_2O_7S$ 533.24, found 533.22. $[\alpha]_D^{20}$ = + 11.5 (*c* = 1, $CHCl_3$).

Synthesis of **MC31**.To a stirred solution of **18** (110 mg, 0.275 mmol) in 2-propanol (1 mL) and dimethylsulfoxide (300 µL), triethylamine (58 µL, 0.41 mmol) was added. After 30 min, **2** (30 mg, 0.137 mmol) was added. The reaction mixture was stirred at r.t. for 142 h, and then concentrated under reduced pressure. The crude was purified by flash chromatography on silica gel (ethyl acetate:methanol 5:1, Rf = 0.2) to give **MC31** (9 mg, 13%) as a white solid. ^{1}H-NMR (400 MHz, $CDCl_3$) δ: 7.71-7.68 (m, 2H, $H_{A'}$), 7.62 (d, J_{D-E} = 9.5 Hz, 1H, H_D), 7.34 (d, J_{C-A} = 8.6 Hz, 1H, H_C), 6.92-6.89 (m, 2H, $H_{B'}$), 6.81 (dd, J_{A-C} = 8.6 Hz, J_{A-B} = 2.2 Hz, 1H, H_A), 6.77 (d, J_{B-A} = 1.9 Hz, 1H, H_B), 6.19 (d, J_{E-D} = 9.5 Hz, 1H, H_E), 4.33-4.30 (m, 1H, H-2), 4.04-3.95 (m, 2H, H-1), 3.79 (s, 3H, -OCH_3), 3.15-3.11 (m, 1H, H-3), 302-2.97 (m, 1H, H-3), 2.92-2.88 (m, 2H, H-9), 2.80-2.76 (m, 2H, H-4), 1.65-1.63 (m, 2H, H-8), 1.42-1.39 (m, 2H, H-5), 1.33-1.26 (m, 4H, H-6, H-7). ^{13}C-NMR (100 MHz, $CDCl_3$) δ: 177.34, 162.69, 161.46, 155.49, 143.78, 128.99, 128.92, 114.14, 113.06, 112.97, 101.63, 70.07, 65.26, 55.49, 50.42, 48.22, 42.54, 28.76, 25.80, 25.65, 25.55. ESI-MS *m/z*: for $[M-H]^+$ calcd. for $C_{25}H_{31}N_2O_7S$ 503.19, found 503.15. $[\alpha]_D^{20}$ = + 94.2 (*c* = 1.1, $CHCl_3$).

Synthesis of **MC32**.To a stirred solution of **19** (90 mg, 0.24 mmol) in 2-propanol (1 mL), triethylamine (50 µL, 0.36 mmol) was added. After 30 min, **1** (30 mg, 0.12 mmol) was added. The reaction mixture was stirred at r.t. for 118 h, then it was concentrated under reduced pressure. The crude was purified by flash chromatography on silica gel (ethyl acetate:methanol 5:1, Rf = 0.2) to give **MC32** (17 mg, 28%) as a white solid. ^{1}H-NMR (400 MHz, $CDCl_3$) δ: 7.79 (ad, J = 8.9 Hz, 1H, H_D), 7.73 (d, J_{B-C} = 8.8 Hz, 1H, H_C), 6.94 (ad, *J* = 8.9 Hz, 1H, H_E), 6.50 (dd, J_{C-B} = 8.8 Hz, J_{C-A} = 2.3 Hz, 1H, H_C), 6.35 (d, *J* = 2.3 Hz, 1H, H_A), 4.54-4.49 (m, 1H, H-2), 4.09-4.00 (m, 2H, H-1), 3.82 (s, 3H, -OCH_3), 3.21-3.12 (m, 2H, H-3), 3.04-3.00 (m, 2H, H-7), 2.93-2.90 (m, 2H, H-4), 2.64 (s, 2H, H_X), 1.97-1.88 (m ,2H, H-6), 1.66-1.60 (m, 2H, H-5), 1.41 (s, 6H, CH_3). ^{13}C-NMR (100 MHz, $CDCl_3$) δ: 191.05, 164.77, 162.76, 161.84, 131.25, 129.16, 128.28, 114.48, 114.25, 109.32, 102.03, 69.94, 66.07, 55.57, 51.19, 48.52, 48.49, 42.23, 26.64, 26.52, 24.29. ESI-MS *m/z*: for $[M-H]^+$ calcd. for $C_{25}H_{33}N_2O_7S$ 505.21, found 505.19. $[\alpha]_D^{20}$ = + 7.3 (*c* = 0.9, $CHCl_3$).

Synthesis of **MC33**.To a stirred solution of **19** (102 mg, 0.275 mmol) in 2-propanol (1 mL) and dimethylsulfoxide (300 µL), triethylamine (58 µL, 0.41 mmol) was added. After 30 min, **2** (30 mg, 0.137 mmol) was added. The reaction mixture was stirred at r.t. for 142 h, then it was concentrated under reduced pressure. The crude was purified by flash chromatography on silica gel (dichloromethane:methanol 5:1, Rf = 0.1) to give **MC33** (12 mg, 18%) as a white solid. ^{1}H-NMR (400 MHz, CD_3OD) δ: 7.85 (d, J_{D-E} = 9.5 Hz, 1H, H_D), 7.77-7.75 (m, 2H, $H_{A'}$), 7.53 (d, J_{C-A} = 8.6 Hz, 1H, H_C), 7.05-7.02 (m, 2H, $H_{B'}$), 6.96 (dd, J_{B-A} = 8.6 Hz, J_{B-C} = 2.4 Hz, 1H, H_B), 6.92 (d, J_{A-C} = 2.3 Hz, 1H, H_A), 6.25 (d, J_{E-D} = 9.5 Hz, 1H, H_E), 4.31-4.25 (m, 1H, H-2), 4.13-4.07 (m, 2H, H-1), 3.86 (s, 3H, -OCH_3), 3.26-3.22 (A part of an ABX system, J_{A-B} = 12.7 Hz, J_{A-X} = 3.1 Hz, 1H, H-3), 3.12-3.09 (m, 1H, H-3), 3.04-3.00 (m, 2H, H-7), 2.88-2.85 (m, 2H, H-4), 1.81-1.73 (m, 2H, H-6), 1.60-1.52 (m, 2H, H-5). ^{13}C-NMR (100 MHz, CD_3OD) δ: 162.96, 161.98, 161.79, 155.54, 144.35, 131.53, 129.20, 128.72, 114.02, 113.10, 112.72, 112.45, 101.31, 70.13, 65.20, 54.97, 49.74, 47.20, 41.82, 26.25, 22.91. ESI-MS *m/z*: for $[M-H]^+$ calcd. for $C_{23}H_{27}N_2O_7S$ 475.16, found 475.12. $[\alpha]_D^{20}$ = + 40.1 (*c* = 1.1, $CHCl_3$).

Synthesis of **MC34**.To a stirred solution of **30** (22 mg, 0.042 mmol) in dichloromethane (1 mL), trifluoroacetic acid (33 µL, 0.42 mmol) was added. The reaction mixture was stirred at r.t. for 4h, then it was concentrated under reduced pressure to give **MC34** (21 mg, quantitative yield) as a white solid. ^{1}H-NMR (400 MHz, $CDCl_3$) δ: 7.88 (s, 1H, $H_{N\alpha}$), 7.18 (d, $J_{A\text{-}B}$ = 8.6 Hz, 2H, H_A), 6.97-6.94 (m, 3H, H_D and H_B), 6.88-6.85 (m, 3H, H_B and H_c), 4.66-4.60 (m, 1H, H-2), 4.35-4.30 (m, 2H, H-1 and H-5), 4.26-4.23 (m, 1H, H-8), 4.07-4.01 (m, 3H, H-6 and H-1'), 3.78 (s, 3H, CH_3), 3.50-3.33 (m, 3H, H-4 and H-7), 3.28-3.09 (m, 3H, H-3 and H-7'). ^{13}C-NMR (100 MHz, $CDCl_3$) δ: 169.05, 158.18, 142.92, 141.65, 130.23, 126.44, 126.42, 121.83, 121.80, 117.16, 116.97, 114.78, 114.69, 69.71, 69.10, 65.10, 64.98, 53.88, 52.11, 50.14, 47.59, 35.19. ESI-MS *m/z*: for $[M\text{-}H]^+$ calcd. for $C_{22}H_{27}N_2O_6$ 415.19, found 415.15. $[\alpha]_D^{20}$ = + 37.3 (*c* = 0.9, $CHCl_3$).

Author contributions

All authors are responsible for revisions and verification and have given approval to the final version of the manuscript.

Declaration of competing interest

The authors declare that they have no known competing financial interests or personal relationships that could have appeared to influence the work reported in this paper.

References

[1] J.B. Regard, I.T. Sato, S.R. Coughlin, Anatomical Profiling of G Protein-Coupled Receptor Expression, Cell. 135 (2008) 561–571. https://doi.org/10.1016/j.cell.2008.08.040.

[2] B.K. Kobilka, Structural insights into adrenergic receptor function and pharmacology, Trends Pharmacol. Sci. 32 (2011) 213–218. https://doi.org/10.1016/j.tips.2011.02.005.

[3] B.K. Velmurugan, R. Baskaran, C.Y. Huang, Detailed insight on β-adrenoceptors as therapeutic targets, Biomed. Pharmacother. 117 (2019) 109039. https://doi.org/10.1016/j.biopha.2019.109039.

[4] A.S. Hauser, M.M. Attwood, M. Rask-Andersen, H.B. Schiöth, D.E. Gloriam, Trends in GPCR drug discovery: New agents, targets and indications, Nat. Rev. Drug Discov. 16 (2017) 829–842. https://doi.org/10.1038/nrd.2017.178.

[5] A.J. Kooistra, S. Mordalski, G. Pándy-Szekeres, M. Esguerra, A. Mamyrbekov, C. Munk, G.M. Keserű, D.E. Gloriam, GPCRdb in 2021: Integrating GPCR sequence, structure and function, Nucleic Acids Res. 49 (2021) D335–D343. https://doi.org/10.1093/nar/gkaa1080.

[6] A.M. LANDS, A. ARNOLD, J.P. MCAULIFF, F.P. LUDUENA, T.G. BROWN, Differentiation of Receptor Systems activated by Sympathomimetic Amines, Nature. 214 (1967) 597–598. https://doi.org/10.1038/214597a0.

[7] B.K. Velmurugan, R. Baskaran, C.Y. Huang, Detailed insight on β-adrenoceptors as therapeutic targets, Biomed. Pharmacother. 117 (2019) 109039. https://doi.org/10.1016/j.biopha.2019.109039.

[8] J.G. Baker, R.G. Wilcox, β-Blockers, heart disease and COPD: current controversies and uncertainties, Thorax. 72 (2017) 271–276. https://doi.org/10.1136/thoraxjnl-2016-208412.

[9] J.A. Salon, D.T. Lodowski, K. Palczewski, The Significance of G Protein-Coupled Receptor Crystallography for Drug Discovery, Pharmacol. Rev. 63 (2011) 901–937. https://doi.org/10.1124/pr.110.003350.

[10] T. Warne, R. Moukhametzianov, J.G. Baker, R. Nehmé, P.C. Edwards, A.G.W. Leslie, G.F.X. Schertler, C.G. Tate, The structural basis for agonist and partial agonist action on a β1-adrenergic receptor, Nature. 469 (2011) 241–245. https://doi.org/10.1038/nature09746.

[11] S.G.F. Rasmussen, H.J. Choi, D.M. Rosenbaum, T.S. Kobilka, F.S. Thian, P.C. Edwards, M. Burghammer, V.R.P. Ratnala, R. Sanishvili, R.F. Fischetti, G.F.X. Schertler, W.I. Weis, B.K. Kobilka, Crystal structure of the human β2 adrenergic G-protein-coupled receptor, Nature. 450 (2007) 383–387. https://doi.org/10.1038/nature06325.

[12] C. Nagiri, K. Kobayashi, A. Tomita, M. Kato, K. Kobayashi, K. Yamashita, T. Nishizawa, A. Inoue, W. Shihoya, O. Nureki, Cryo-EM structure of the β3-adrenergic receptor reveals the molecular basis of subtype selectivity, Mol. Cell. 81 (2021) 3205-3215.e5. https://doi.org/10.1016/j.molcel.2021.06.024.

[13] M.M. Scharf, M. Bünemann, J.G. Baker, P. Kolb, Comparative Docking to Distinct G Protein–Coupled Receptor Conformations Exclusively Yields Ligands with Agonist Efficacy, Mol. Pharmacol. 96 (2019) 851–861. https://doi.org/10.1124/mol.119.117515.

[14] D.R. Weiss, S. Ahn, M.F. Sassano, A. Kleist, X. Zhu, R. Strachan, B.L. Roth, R.J. Lefkowitz, B.K. Shoichet, Conformation guides molecular efficacy in docking screens of activated β-2 adrenergic G protein coupled receptor, ACS Chem. Biol. 8 (2013) 1018–1026. https://doi.org/10.1021/cb400103f.

[15] H.C.S. Chan, S. Filipek, S. Yuan, The Principles of Ligand Specificity on beta-2-adrenergic receptor, Sci. Rep. 6 (2016) 1–11. https://doi.org/10.1038/srep34736.

[16] Y. Du, N.M. Duc, S.G.F. Rasmussen, D. Hilger, X. Kubiak, L. Wang, J. Bohon, H.R. Kim, M. Wegrecki, A. Asuru, K.M. Jeong, J. Lee, M.R. Chance, D.T. Lodowski, B.K. Kobilka, K.Y. Chung, Assembly of a GPCR-G Protein Complex, Cell. 177 (2019) 1232-1242.e11. https://doi.org/10.1016/j.cell.2019.04.022.

[17] C. Nagiri, K. Kobayashi, A. Tomita, M. Kato, K. Kobayashi, K. Yamashita, T. Nishizawa, A. Inoue, W. Shihoya, O. Nureki, Cryo-EM structure of the β3-adrenergic receptor reveals the molecular basis of subtype selectivity, Mol. Cell. 81 (2021) 3205-3215.e5. https://doi.org/10.1016/j.molcel.2021.06.024.

[18] J.S. Mason, A. Bortolato, M. Congreve, F.H. Marshall, New insights from structural biology into the druggability of G protein-coupled receptors, Trends Pharmacol. Sci. 33 (2012) 249–260. https://doi.org/10.1016/j.tips.2012.02.005.

[19] A. Manglik, T.H. Kim, M. Masureel, C. Altenbach, Z. Yang, D. Hilger, M.T. Lerch, T.S. Kobilka, F.S. Thian, W.L. Hubbell, R.S. Prosser, B.K. Kobilka, Structural Insights into the Dynamic Process of β 2 -Adrenergic Receptor Signaling, Cell. 161 (2015) 1101–1111. https://doi.org/10.1016/j.cell.2015.04.043.

[20] D. Wacker, R.C. Stevens, B.L. Roth, How Ligands Illuminate GPCR Molecular Pharmacology, Cell. 170 (2017) 414–427. https://doi.org/10.1016/j.cell.2017.07.009.

[21] T. Warne, P.C. Edwards, A.S. Doré, A.G.W. Leslie, C.G. Tate, Molecular basis for high-affinity agonist binding in GPCRs, Science. 364 (2019) 775–778.

https://doi.org/10.1126/science.aau5595.

[22] M. Masureel, Y. Zou, L.P. Picard, E. van der Westhuizen, J.P. Mahoney, J.P.G.L.M. Rodrigues, T.J. Mildorf, R.O. Dror, D.E. Shaw, M. Bouvier, E. Pardon, J. Steyaert, R.K. Sunahara, W.I. Weis, C. Zhang, B.K. Kobilka, Structural insights into binding specificity, efficacy and bias of a β 2 AR partial agonist, Nat. Chem. Biol. 14 (2018) 1059–1066. https://doi.org/10.1038/s41589-018-0145-x.

[23] M. Vass, A.J. Kooistra, T. Ritschel, R. Leurs, I.J. de Esch, C. de Graaf, Molecular interaction fingerprint approaches for GPCR drug discovery, Curr. Opin. Pharmacol. 30 (2016) 59–68. https://doi.org/10.1016/j.coph.2016.07.007.

[24] D.R. Weiss, S. Ahn, M.F. Sassano, A. Kleist, X. Zhu, R. Strachan, B.L. Roth, R.J. Lefkowitz, B.K. Shoichet, Conformation Guides Molecular Efficacy in Docking Screens of Activated β-2 Adrenergic G Protein Coupled Receptor, ACS Chem. Biol. 8 (2013) 1018–1026. https://doi.org/10.1021/cb400103f.

[25] M.M. Scharf, M. Zimmermann, F. Wilhelm, R. Stroe, M. Waldhoer, P. Kolb, A Focus on Unusual ECL2 Interactions Yields β2 -Adrenergic Receptor Antagonists with Unprecedented Scaffolds., ChemMedChem. 15 (2020) 882–890. https://doi.org/10.1002/cmdc.201900715.

[26] C. Hoffmann, M.R. Leitz, S. Oberdorf-Maass, M.J. Lohse, K.N. Klotz, Comparative pharmacology of human β-adrenergic receptor subtypes - Characterization of stably transfected receptors in CHO cells, Naunyn. Schmiedebergs. Arch. Pharmacol. 369 (2004) 151–159. https://doi.org/10.1007/s00210-003-0860-y.

[27] J.G. Baker, The selectivity of β-adrenoceptor antagonists at the human β1, β2 and β3 adrenoceptors, Br. J. Pharmacol. 144 (2005) 317–322. https://doi.org/10.1038/sj.bjp.0706048.

[28] S.D. Edmondson, C. Zhu, N.F. Kar, J. Di Salvo, H. Nagabukuro, B. Sacre-Salem, K. Dingley, R. Berger, S.D. Goble, G. Morriello, B. Harper, C.R. Moyes, D.-M. Shen, L. Wang, R. Ball, A. Fitzmaurice, T. Frenkl, L.N. Gichuru, S. Ha, A.L. Hurley, N. Jochnowitz, D. Levorse, S. Mistry, R.R. Miller, J. Ormes, G.M. Salituro, A. Sanfiz, A.S. Stevenson, K. Villa, B. Zamlynny, S. Green, M. Struthers, A.E. Weber, Discovery of Vibegron: A Potent and Selective β 3 Adrenergic Receptor Agonist for the Treatment of Overactive Bladder, J. Med. Chem. 59 (2016) 609–623. https://doi.org/10.1021/acs.jmedchem.5b01372.

[29] C. Du, X. Xie, G protein-coupled receptors as therapeutic targets for multiple sclerosis, Cell Res. 22 (2012) 1108–1128. https://doi.org/10.1038/cr.2012.87.

[30] L. Qian, H. Wu, S.-H. Chen, D. Zhang, S.F. Ali, L. Peterson, B. Wilson, R.-B. Lu, J.-S. Hong, P.M. Flood, β2-Adrenergic Receptor Activation Prevents Rodent Dopaminergic Neurotoxicity by Inhibiting Microglia via a Novel Signaling Pathway, J. Immunol. 186 (2011) 4443–4454. https://doi.org/10.4049/jimmunol.1002449.

[31] R. Lappano, M. Maggiolini, G protein-coupled receptors: Novel targets for drug discovery in cancer, Nat. Rev. Drug Discov. 10 (2011) 47–60. https://doi.org/10.1038/nrd3320.

[32] S.L. Rains, C.N. Amaya, B.A. Bryan, Beta-adrenergic receptors are expressed across diverse cancers, Oncoscience. 4 (2017) 95–105. https://doi.org/10.18632/oncoscience.357.

[33] M. Coelho, C. Soares-Silva, D. Brandão, F. Marino, M. Cosentino, L. Ribeiro, β-Adrenergic modulation of cancer cell proliferation: available evidence and clinical perspectives, J. Cancer Res. Clin. Oncol. 143 (2017) 275–291.

https://doi.org/10.1007/s00432-016-2278-1.

[34] M. Dal Monte, M. Calvani, M. Cammalleri, C. Favre, L. Filippi, P. Bagnoli, β-Adrenoceptors as drug targets in melanoma: novel preclinical evidence for a role of β 3 -adrenoceptors, Br. J. Pharmacol. 176 (2019) 2496–2508. https://doi.org/10.1111/bph.14552.

[35] R.D. Gillis, E. Botteri, A. Chang, A.I. Ziegler, N.C. Chung, C.K. Pon, D.M. Shackleford, B.K. Andreassen, M.L. Halls, J.G. Baker, E.K. Sloan, Carvedilol blocks neural regulation of breast cancer progression in vivo and is associated with reduced breast cancer mortality in patients, Eur. J. Cancer. 147 (2021) 106–116. https://doi.org/10.1016/j.ejca.2021.01.029.

[36] D.M. Rosenbaum, V. Cherezov, M.A. Hanson, S.G.F. Rasmussen, F.S. Thian, T.S. Kobilka, H.-J. Choi, X.-J. Yao, W.I. Weis, R.C. Stevens, B.K. Kobilka, GPCR Engineering Yields High-Resolution Structural Insights into β 2 -Adrenergic Receptor Function, Science. 318 (2007) 1266–1273. https://doi.org/10.1126/science.1150609.

[37] V. Cherezov, D.M. Rosenbaum, M.A. Hanson, S.G.F. Rasmussen, F.S. Thian, T.S. Kobilka, H.-J. Choi, P. Kuhn, W.I. Weis, B.K. Kobilka, R.C. Stevens, High-Resolution Crystal Structure of an Engineered Human β 2 -Adrenergic G Protein–Coupled Receptor, Science. 318 (2007) 1258–1265. https://doi.org/10.1126/science.1150577.

[38] M.Y.S. Kalani, N. Vaidehi, S.E. Hall, R.J. Trabanino, P.L. Freddolino, M.A. Kalani, W.B. Floriano, V.W.T. Kam, W.A. Goddard, The predicted 3D structure of the human D2 dopamine receptor and the binding site and binding affinities for agonists and antagonists, Proc. Natl. Acad. Sci. U. S. A. 101 (2004) 3815–3820. https://doi.org/10.1073/pnas.0400100101.

[39] C.J. Dickson, V. Hornak, C. Velez-Vega, D.J.J. McKay, J. Reilly, D.A. Sandham, D. Shaw, R.A. Fairhurst, S.J. Charlton, D.A. Sykes, R.A. Pearlstein, J.S. Duca, Uncoupling the Structure–Activity Relationships of β2 Adrenergic Receptor Ligands from Membrane Binding, J. Med. Chem. 59 (2016) 5780–5789. https://doi.org/10.1021/acs.jmedchem.6b00358.

[40] D. Wacker, G. Fenalti, M.A. Brown, V. Katritch, R. Abagyan, V. Cherezov, R.C. Stevens, Conserved Binding Mode of Human β 2 Adrenergic Receptor Inverse Agonists and Antagonist Revealed by X-ray Crystallography, J. Am. Chem. Soc. 132 (2010) 11443–11445. https://doi.org/10.1021/ja105108q.

[41] J.W. Black, W.A.M. Duncan, R.G. Shanks, Comparison of some properties of pronethal and propranolol, Br. J. Pharmacol. Chemother. 25 (1965) 577–591. https://doi.org/10.1111/j.1476-5381.1965.tb01782.x.

[42] M.P. Stapleton, Sir James black and propranolol the role of the basic sciences in the history of cardiovascular pharmacology, Texas Hear. Inst. J. 24 (1997) 336–342.

[43] J.R.S. Arch, A.T. Ainsworth, M.A. Cawthorne, V. Piercy, M. V. Sennitt, V.E. Thody, C. Wilson, S. Wilson, Atypical β-adrenoceptor on brown adipocytes as target for anti-obesity drugs, Nature. 309 (1984) 163–165. https://doi.org/10.1038/309163a0.

[44] L.J. Emorine, S. Marullo, M.-M. Briend-Sutren, G. Patey, K. Tate, C. Delavier-Klutchko, A.D. Strosberg, Molecular Characterization of the Human β 3 -Adrenergic Receptor, Science. 245 (1989) 1118–1121. https://doi.org/10.1126/science.2570461.

[45] J.R.S. Arch, A.J. Kaumann, β3 and Atypical β-Adrenoceptors, Med. Res. Rev. 13 (1993) 663–729. https://doi.org/10.1002/med.2610130604.

[46] H. Cernecka, C. Sand, M.C. Michel, The Odd Sibling: Features of β 3 -Adrenoceptor Pharmacology, Mol. Pharmacol. 86 (2014) 479–484.

https://doi.org/10.1124/mol.114.092817.

[47] M.G. Ursino, V. Vasina, E. Raschi, F. Crema, F. De Ponti, The β3-adrenoceptor as a therapeutic target: Current perspectives, Pharmacol. Res. 59 (2009) 221–234. https://doi.org/10.1016/j.phrs.2009.01.002.

[48] G. Schena, M.J. Caplan, Everything You Always Wanted to Know about β3-AR * (* But Were Afraid to Ask), Cells. 8 (2019) 357. https://doi.org/10.3390/cells8040357.

[49] K. Okeke, S. Angers, M. Bouvier, M.C. Michel, Agonist-induced desensitisation of β 3 - adrenoceptors: Where, when, and how?, Br. J. Pharmacol. 176 (2019) 2539–2558. https://doi.org/10.1111/bph.14633.

[50] S. Ravez, O. Castillo-Aguilera, P. Depreux, L. Goossens, Quinazoline derivatives as anticancer drugs: A patent review (2011-present), Expert Opin. Ther. Pat. 25 (2015) 789–804. https://doi.org/10.1517/13543776.2015.1039512.

[51] C.R. Chapple, L. Cardozo, V.W. Nitti, E. Siddiqui, M.C. Michel, Mirabegron in overactive bladder: A review of efficacy, safety, and tolerability, Neurourol. Urodyn. 33 (2014) 17–30. https://doi.org/10.1002/nau.22505.

[52] M. Calvani, A. Subbiani, M. Vignoli, C. Favre, Spotlight on ROS and β 3-Adrenoreceptors Fighting in Cancer Cells, Oxid. Med. Cell. Longev. (2019) 6346529. https://doi.org/10.1155/2019/6346529.

[53] G. Bruno, F. Cencetti, A. Pini, A. Tondo, D. Cuzzubbo, F. Fontani, V. Strinna, A.M. Buccoliero, G. Casazza, C. Donati, L. Filippi, P. Bruni, C. Favre, M. Calvani, β3-adrenoreceptor blockade reduces tumor growth and increases neuronal differentiation in neuroblastoma via SK2/S1P2 modulation, Oncogene. 39 (2020) 368–384. https://doi.org/10.1038/s41388-019-0993-1.

[54] M. Calvani, G. Bruno, M. Dal Monte, R. Nassini, F. Fontani, A. Casini, L. Cavallini, M. Becatti, F. Bianchini, F. De Logu, G. Forni, G. la Marca, L. Calorini, P. Bagnoli, P. Chiarugi, A. Pupi, C. Azzari, P. Geppetti, C. Favre, L. Filippi, β3-Adrenoceptor as a potential immuno-suppressor agent in melanoma, 2019. https://doi.org/10.1111/bph.14660.

[55] M. Calvani, L. Cavallini, A. Tondo, V. Spinelli, L. Ricci, A. Pasha, G. Bruno, D. Buonvicino, E. Bigagli, M. Vignoli, F. Bianchini, L. Sartiani, M. Lodovici, R. Semeraro, F. Fontani, F. De Logu, M. Dal Monte, P. Chiarugi, C. Favre, L. Filippi, β 3-Adrenoreceptors Control Mitochondrial Dormancy in Melanoma and Embryonic Stem Cells, Oxid. Med. Cell. Longev. (2018) 6816508. https://doi.org/10.1155/2018/6816508.

[56] L. Manara, D. Badone, M. Baroni, G. Boccardi, R. Cecchi, T. Croci, A. Giudice, U. Guzzi, M. Landi, G. Fur, Functional identification of rat atypical β-adrenoceptors by the first β3-selective antagonists, aryloxypropanolaminotetralins, Br. J. Pharmacol. 117 (1996) 435–442. https://doi.org/10.1111/j.1476-5381.1996.tb15209.x.

[57] M. Sato, T. Horinouchi, D.S. Hutchinson, B.A. Evans, R.J. Summers, Ligand-directed signaling at the β3-adrenoceptor produced by 3-(2-ethylphenoxy)-1-[(1,S)-1,2,3,4-tetrahydronapth-1-ylamino]-2S-2-propanol oxalate (SR59230A) relative to receptor agonists, Mol. Pharmacol. 72 (2007) 1359–1368. https://doi.org/10.1124/mol.107.035337.

[58] J.G. Baker, The selectivity of β-adrenoceptor agonists at human β 1-, β 2- and β 3-adrenoceptors: RESEARCH PAPER, Br. J. Pharmacol. 160 (2010) 1048–1061. https://doi.org/10.1111/j.1476-5381.2010.00754.x.

[59] B.A. Evans, M. Sato, M. Sarwar, D.S. Hutchinson, R.J. Summers, Ligand-directed

signalling at beta-adrenoceptors., Br. J. Pharmacol. 159 (2010) 1022–38. https://doi.org/10.1111/j.1476-5381.2009.00602.x.

[60] R. Lamichhane, J.J. Liu, K.L. White, V. Katritch, R.C. Stevens, K. Wüthrich, D.P. Millar, Biased Signaling of the G-Protein-Coupled Receptor β2AR Is Governed by Conformational Exchange Kinetics, Structure. 28 (2020) 371-377.e3. https://doi.org/10.1016/j.str.2020.01.001.

[61] L.-P. Picard, A.M. Schönegge, M.J. Lohse, M. Bouvier, Bioluminescence resonance energy transfer-based biosensors allow monitoring of ligand- and transducer-mediated GPCR conformational changes, Commun. Biol. 1 (2018) 106. https://doi.org/10.1038/s42003-018-0101-z.

[62] D. Schmidt, J. Gunera, J.G. Baker, P. Kolb, Similarity- and Substructure-Based Development of β 2 -Adrenergic Receptor Ligands Based on Unusual Scaffolds, ACS Med. Chem. Lett. 8 (2017) 481–485. https://doi.org/10.1021/acsmedchemlett.6b00363.

[63] F. Chevillard, H. Rimmer, C. Betti, E. Pardon, S. Ballet, N. van Hilten, J. Steyaert, W.E. Diederich, P. Kolb, Binding-Site Compatible Fragment Growing Applied to the Design of β 2 -Adrenergic Receptor Ligands, J. Med. Chem. 61 (2018) 1118–1129. https://doi.org/10.1021/acs.jmedchem.7b01558.

[64] N. Shakya, K.K. Roy, A.K. Saxena, Substituted 1,2,3,4-tetrahydroquinolin-6-yloxypropanes as β3-adrenergic receptor agonists: Design, synthesis, biological evaluation and pharmacophore modeling, Bioorg. Med. Chem. 17 (2009) 830–847. https://doi.org/10.1016/j.bmc.2008.11.030.

[65] M. McGann, FRED pose prediction and virtual screening accuracy, J. Chem. Inf. Model. 51 (2011) 578–596. https://doi.org/10.1021/ci100436p.

[66] M.R. McGann, H.R. Almond, A. Nicholls, J.A. Grant, F.K. Brown, Gaussian docking functions, Biopolymers. 68 (2003) 76–90. https://doi.org/10.1002/bip.10207.

[67] P.C.D. Hawkins, A. Nicholls, Conformer generation with OMEGA: Learning from the data set and the analysis of failures, J. Chem. Inf. Model. 52 (2012) 2919–2936. https://doi.org/10.1021/ci300314k.

[68] P.C.D. Hawkins, A.G. Skillman, G.L. Warren, B.A. Ellingson, M.T. Stahl, Conformer generation with OMEGA: Algorithm and validation using high quality structures from the protein databank and cambridge structural database, J. Chem. Inf. Model. 50 (2010) 572–584. https://doi.org/10.1021/ci100031x.

[69] A.J. Kooistra, R. Leurs, I.J.P. De Esch, C. De Graaf, Structure-based prediction of g-protein-coupled receptor ligand function: A β-adrenoceptor case study, J. Chem. Inf. Model. 55 (2015) 1045–1061. https://doi.org/10.1021/acs.jcim.5b00066.

[70] M.G. Perrone, A. Scilimati, β3-Adrenoceptor ligand development history through patent review, Expert Opin. Ther. Pat. 21 (2011) 505–536. https://doi.org/10.1517/13543776.2011.561316.

[71] M.G. Perrone, A. Scilimati, β 3 -Adrenoceptor agonists and (Antagonists as) inverse agonists. History, perspective, constitutive activity, and stereospecific binding, 1st ed., Elsevier Inc., 2010. https://doi.org/10.1016/B978-0-12-381298-8.00011-3.

[72] M.G. Perrone, E. Santandrea, L. Bleve, P. Vitale, N.A. Colabufo, R. Jockers, F.M. Milazzo, A.F. Sciarroni, A. Scilimati, Stereospecific synthesis and bio-activity of novel β3-adrenoceptor agonists and inverse agonists, Bioorganic Med. Chem. 16 (2008) 2473–2488. https://doi.org/10.1016/j.bmc.2007.11.060.

[73] A. Ishchenko, B. Stauch, G.W. Han, A. Batyuk, A. Shiriaeva, C. Li, N. Zatsepin, U. Weierstall, W. Liu, E. Nango, T. Nakane, R. Tanaka, K. Tono, Y. Joti, S. Iwata, I. Moraes, C. Gati, V. Cherezov, Toward G protein-coupled receptor structure-based drug design using X-ray lasers, IUCrJ. 6 (2019) 1106–1119. https://doi.org/10.1107/S2052252519013137.

[74] M. Wheatley, D. Wootten, M. Conner, J. Simms, R. Kendrick, R. Logan, D. Poyner, J. Barwell, Lifting the lid on GPCRs: the role of extracellular loops, Br. J. Pharmacol. 165 (2012) 1688–1703. https://doi.org/10.1111/j.1476-5381.2011.01629.x.

[75] Z.A. Bredikhina, A. V. Kurenkov, D.B. Krivolapov, A.A. Bredikhin, Synthesis of all of the stereoisomers of β3-adrenoceptor antagonist SR 59230 based on the spontaneous resolution of 3-(2-ethylphenoxy)propane-1,2-diol, Tetrahedron: Asymmetry. 27 (2016) 467–474. https://doi.org/10.1016/j.tetasy.2016.05.001.

[76] J.G. Baker, L.A. Adams, K. Salchow, S.N. Mistry, R.J. Middleton, S.J. Hill, B. Kellam, Synthesis and Characterization of High-Affinity 4,4-Difluoro-4-bora-3a,4a-diaza- s -indacene-Labeled Fluorescent Ligands for Human β-Adrenoceptors, J. Med. Chem. 54 (2011) 6874–6887. https://doi.org/10.1021/jm2008562.

[77] K.K. Roy, A.K. Saxena, Structural Basis for the β-Adrenergic Receptor Subtype Selectivity of the Representative Agonists and Antagonists, J. Chem. Inf. Model. 51 (2011) 1405–1422. https://doi.org/10.1021/ci2000874.

[78] P. Prathipati, A.K. Saxena, Characterization of β3-adrenergic receptor: determination of pharmacophore and 3D QSAR model for β3 adrenergic receptor agonism, J. Comput. Aided. Mol. Des. 19 (2005) 93–110. https://doi.org/10.1007/s10822-005-1558-7.

[79] B. Selvam, J. Wereszczynski, I.G. Tikhonova, Comparison of Dynamics of Extracellular Accesses to the β1 and β2 Adrenoceptors Binding Sites Uncovers the Potential of Kinetic Basis of Antagonist Selectivity, Chem. Biol. Drug Des. 80 (2012) 215–226. https://doi.org/10.1111/j.1747-0285.2012.01390.x.

[80] J.G. Baker, A study of antagonist affinities for the human histamine H 2 receptor, Br. J. Pharmacol. 153 (2008) 1011–1021. https://doi.org/10.1038/sj.bjp.0707644.

[81] R.P. Stephenson, A modification of receptor theory, Br. J. Pharmacol. Chemother. 11 (1956) 379–393. https://doi.org/10.1111/j.1476-5381.1956.tb00006.x.